Chemistry–A European Journal
Research Article
doi.org/10.1002/chem.202400580
Chemistry Europe
European Chemical Societies Publishing
www.chemeurj.org

Intramolecularly O,N,O-Coordinated Tin(II) Salts: Syntheses, Structures, Cyclization, and Transition Metal Complexation

Hazem Alnasr,[a] David Mroß,[a] André Platzek,[a] Bastian Nayyar,[a] Tomáš Řičica,[a, b] Dieter Schollmeyer,[c] Roman Jambor,*[b] Alexander Hoffmann,*[d] and Klaus Jurkschat*[a]

Dedicated to Prof. Michael Veith on the occasion of his 80th birthday

We report the syntheses of tin(II) salts of the types $[L^1SnX]SnX_3$ [L^1 = 2,6-{(*i*-PrO)$_2$(O)P}$_2$C$_5$H$_3$N: **1**, X=Cl; **2**, X=Br], $[L^2SnCl]SnCl_3$ [L^2 = 2-{(*i*-PrO)Ph(O)P}-6-{(*i*-PrO)$_2$(O)P}C$_5$H$_3$N: **3**], $[L^3SnX]SnX_3$ [L^3 = 2,6-{MeO(O)C}$_2$C$_5$H$_3$N: **4**, X=Cl; **5**, X=Br], $[L^4SnX]SnX_3$ [L^4 = 2,6-{Et$_2$N(O)C}$_2$C$_5$H$_3$N: **6**, X=Cl; **7**, X=Br]. These compounds were obtained by addition of SnX_2 to the corresponding ligand inducing autoionization of the respective tin(II) halide. The thermal stability of **1**, **3**, and **4** was elucidated, giving, under ester cleavage and cyclisation, the tin(II) derivatives **8**–**12**. The reaction of $[L^1SnCl]SnCl_3$ (**1**) with $W(CO)_4(thf)_2$ afforded the tungsten tetracarbonyl complex $[\{L^1SnCl\}\{SnCl_3\}W(CO)_4]$ (**13**), representing the first example in which a tin(II) stannate anion and a tin(II) stannylium cation simultaneously coordinate to a transition metal centre. The compounds were characterized by single crystal X-ray diffraction analyses and in part by elemental analyses, IR and NMR spectroscopy, electrospray ionization mass spectrometry. DFT calculations accompany the experimental work.

Introduction

The chemistry of heavier carbene homologues has been extensively studied in the last decades.[1] Like p-block element cations in general,[1f] in recent years subvalent group XIV element cations in particular have attracted considerable interest. This is due to the assumption that the positive charge increases the electrophilicity of the metal centre, while the lone pair keeps its nucleophilic character.[2] Hence, such compounds are a playground for fundamental studies concerning the bonding and reactivity of such species. Jutzi and coworkers opened this field in the early nineteen eighties and showed that it is possible to stabilize cations of the type $[RM^{(II)}]^+$ (M=Si, Ge, Sn) by utilization of bulky cyclopentadienyl groups.[3] Moreover, these studies revealed that covalently bound substituents on cationic centres of heavier group XIV elements are required to provide electronic stabilization to protect positively charged species from reactions with solvents and counter anions.[4] A valuable approach in this regard represents the concept of Lewis base-mediated autoionization of MCl_2 giving salts containing $[MCl]^+$ cations and $[MCl_3]^-$ anions. Scheme 1 illustrates randomly selected (not complete) prominent examples of such complexes.

In 2008, Stalke et al. reported the tin$^{(II)}$ complex **A** based on diphenyl(2-picolyl)phosphane.[5] Roesky et al., and shortly thereafter we ourselves and Fischer et al., published diketiminato-supported germanium and tin salts (**B**), which are stabilized by a tridentate pincer-type architecture.[6] In a similar approach, Jambor et al. reported closely related complexes of types **C** and **I** by the use of Schiff base-type chelating ligands as did Majumdar and co-workers for similar compounds.[7] Autoionization of $SnCl_2$ was also achieved by employing an *o*-phenylene-backboned organoarsane ligand, as illustrated in **D**.[8] Notably, Reid and co-workers demonstrated that the corresponding organophosphane gave the simple $SnCl_2$ complex as a Cl-bridged dimer.[8] We published the complex **E** containing a redox-active ferrocene moiety.[9a] Driess et al. presented the $[SnBr]^+$ cation **F** stabilized by a xanthene-backboned bisphosphinidene[9b] whereas Inoue et al. studied tin cations of types **G**[9c] and **H**[9d]. Tetrylenium salts with the cations stabilized by a bulky carbazolyl substituent were reported by Hinz.[9e] Troponimines,[9f] β-diketiminates,[9g] bipyridine,[9h] *p*-dimethylaminopyridine,[9i] secondary amides,[9j] crown ethers,[9k] and cryptands[9l] were also used as ligands respectively substituents to stabilize Sn$^{(II)}$ cations. Finally, Pietschnig and co-

[a] H. Alnasr, D. Mroß, A. Platzek, B. Nayyar, T. Řičica, K. Jurkschat
Technische Universität Dortmund, Fakultät für Chemie und Chemische Biologie, 44221 Dortmund, Germany
E-mail: klaus.jurkschat@tu-dortmund.de
[b] T. Řičica, R. Jambor
Department of General and Inorganic Chemistry, Faculty of Chemical Technology, University of Pardubice, Studentská 573, 53210 Pardubice, Czech Republic
E-mail: roman.jambor@upce.cz
[c] D. Schollmeyer
Johannes Gutenberg-Universität Mainz, Department Chemie, Zentrale Analytik,Duesbergweg 10–14, 55099 Mainz, Germany
[d] A. Hoffmann
RWTH Aachen University, Institut für Anorganische Chemie, Landoltweg 1a, 52074 Aachen, Germany
E-mail: alexander.hoffmann@ac.rwth-aachen.de

Supporting information for this article is available on the WWW under https://doi.org/10.1002/chem.202400580

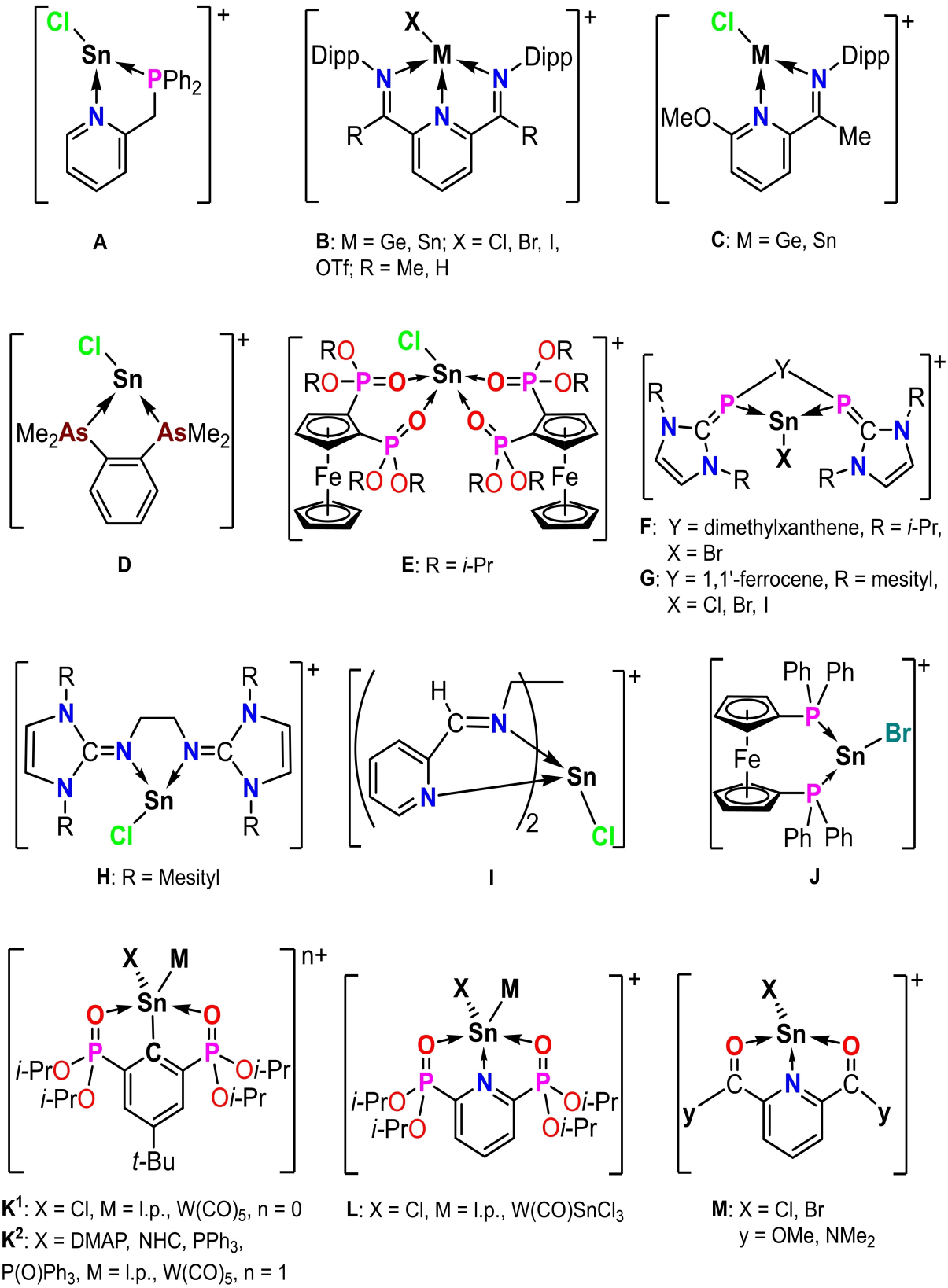

Scheme 1. Examples of group 14 donor-stabilized $M^{(II)+}$ cations **A**-**J**, the heteroleptic organostannylenes K^1 and K^2, and of the novel complexes **L** and **M** reported in this manuscript and being isoelectronic to K^1, K^2. The MX_3^- (for **A**-**I**, K^2, **L**, **M**) and $AlBrCl_3^-$ (for **J**) counter anions are omitted for clarity.

workers found 1,1′-bis(diphenylphosphino)ferrocene, dppf, to ionize $SnBr_2$ under assistance of the Lewis acid $AlCl_3$, giving the complex **J**.[9m]

In continuation of our ongoing interest in subvalent organotin compounds of types $\mathbf{K^1}$ and $\mathbf{K^2}$ including tin$^{(II)}$ cations,[10] the concept of isoelectronic species in mind (C^- is isoelectronic with N), and inspired by the work of Novosad and co-workers[11a] reporting the complexes $[2,6\text{-}\{Ph_2(O)P\}_2C_5H_3NSnCl_3]SnCl_5$, herein we present the novel O,N,O-coordinated tin$^{(II)}$ complexes of types **L** and **M**, and of related derivatives, and discuss their structures in the solid state and in part in solution. The influence of the substituent X as well as of the ligand-backbone on the structures is elucidated, helping to expand the knowledge of this exciting subchapter of group XIV element chemistry. Notably, during the writing of this manuscript, a paper appeared reporting the use of the ligand 2,6-$[(i\text{-}PrO)_2(O)P]_2C_5H_3N$ as chelators for trivalent f-elements.[11b] And most recently, we and others, in a parallel study, reported the use of phosphorus-containing non-symmetric N,N′,O-chelating ligands for the stabilization of $Sn(II)^+$ cations.[11c] Last but not least, a recent review by Inoue et al. illustrates the ongoing interest in donor-stabilized main group element cations.[11d]

Results and Discussion

Synthesis of the Pyridine-backboned Ligands $L^1$and L^2, and the Intermediate L^{2i}

The ligands $\mathbf{L^1}$ and $\mathbf{L^2}$ were synthesized according to the Hirao cross-coupling reaction[11] (Scheme 2).

Heating 2,6-dibromopyridine with two molar equiv. diisopropyl phosphite, triethyl amine, palladium acetate, and 1,1′-bis(diphenylphosphino) ferrocene (dppf) in acetonitrile at 90 °C for 24 h gave 2,6-$\{P(O)(OiPr)_2\}_2C_5H_3N$, $\mathbf{L^1}$, in high yield. Performing the reaction in a one-to-one stoichiometry provided the mono-phosphorylated pyridine intermediate 6-Br-2-$[P(O)(O\text{-}iPr)_2]C_5H_4N$, $\mathbf{L^{2i}}$. Subsequent reaction of the latter with one molar equiv. diisopropyl phosphite gave the unsymmetrically substituted ligand 2-$[(i\text{-}PrO)Ph(O)P]$-6-$[(i\text{-}PrO)_2(O)P]C_5H_3N$, $\mathbf{L^2}$. The ligands $\mathbf{L^1}$ and $\mathbf{L^2}$ as well as the intermediate $\mathbf{L^{2i}}$ are brownish solid materials. They are soluble in common organic solvents such as hexane, THF, chloroform, dichloromethane, and toluene. Their $^{31}P\{^1H\}$ NMR spectra in C_6D_6 ($\mathbf{L^1}$ and $\mathbf{L^2}$) and $CDCl_3$ solutions ($\mathbf{L^{2i}}$), respectively, show singlet resonances at δ 7.7 ($\mathbf{L^1}$), δ 22.3 [$\mathbf{L^2}$, *P*(O)(O*i*Pr)Ph] and δ 7.2 [$\mathbf{L^2}$, *P*(O)(O*i*Pr)$_2$], and δ 6.5 ppm ($\mathbf{L^{2i}}$). The ^1H and ^{13}C NMR spectra given in the experimental part further support the identity of these compounds.

The intermediate $\mathbf{L^{2i}}$ crystalized from its solution composed of methyl acetate and *iso*-hexane in the monoclinic space group $P2_1/n$ with four molecules per unit cell. Figure 1 shows a cut-out of the crystal structure and the caption contains selected interatomic distances and angles.

The P1 centre shows a distorted tetrahedral environment (average angle 109.2°) with angles ranging from 117.18(11) (O1-P1-O2) to 101.16(10)° (O2-P1-C6). A remarkable feature of the crystal structure is the intermolecular P=O→Br (O1 A→Br) interaction at a distance of 3.017(17) Å being shorter than the sum of the van der Waals radii (3.35 Å)[12a–c] of the atoms involved; a case of halogen bond being a topic of high interest in the last decade.[12d–f]

Synthesis and Structures of the P-containing tin(II) Complexes 1-3

The treatment of the ligand 2,6-$[P(O)(OiPr)_2]_2C_5H_3N$ ($\mathbf{L^1}$) with SnX_2 in toluene at room temperature gave the novel tin(II) complexes $[L^1SnX]SnX_3$ (**1**, X=Cl; **2**, X=Br) as air-stable solid materials in good to excellent yields (Scheme 3).

They show good solubility in common organic solvents such as toluene, benzene and THF. Single crystals of **1** and **2** suitable for X-ray diffraction analysis were obtained by slow evaporation of their saturated toluene solutions. They crystallized in the orthorhombic space group *P*bca (**1**) and the monoclinic space group *C*2/c (**2**), both with eight ion pairs in the unit cell. On the other hand, at 263 K compound **1**

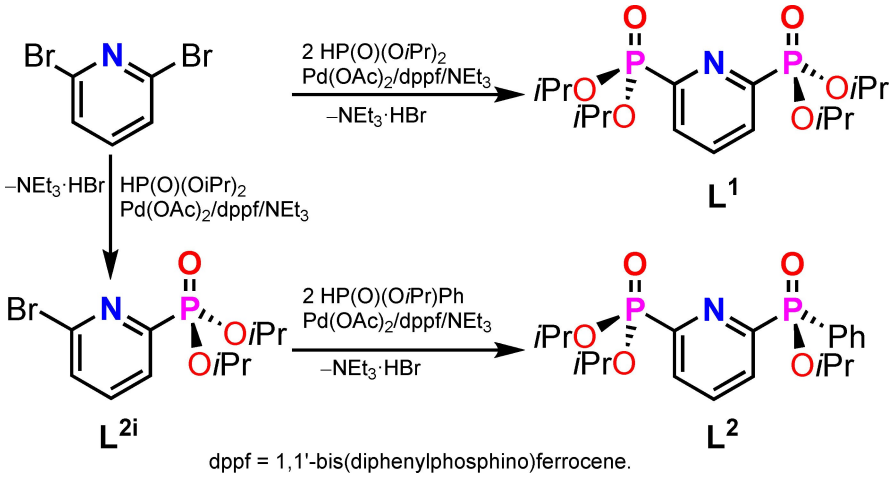

Scheme 2. Synthesis of the pyridine-backboned ligands $\mathbf{L^1}$ and $\mathbf{L^2}$, and of the intermediate $\mathbf{L^{2i}}$.

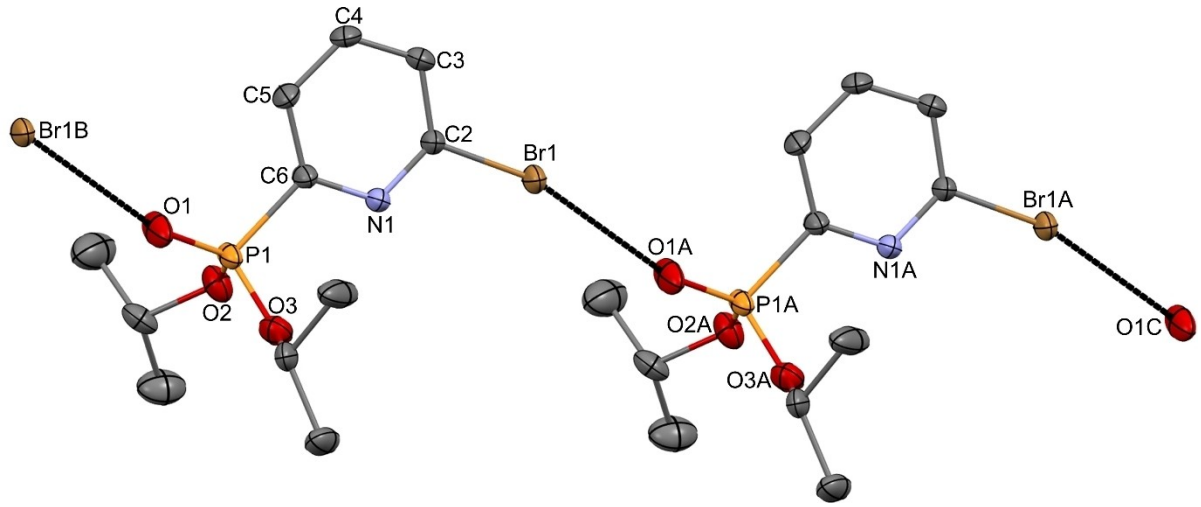

Figure 1. Cut-out of the crystal structure of compound L^{2i} (ORTEP presentations at 50% probability of the depicted atoms and atom numbering scheme). The hydrogen atoms have been omitted. Selected interatomic distances (Å): P1-O1 1.4584(17), P1-O2 1.5598(17), P1-O3 1.5702(17), P1-C6 1.803(2), Br1-O1 A 3.017(17). Selected interatomic angles (°): N1-C6-P1 116.07(14), P1-C6-C5 120.77(16), O1-P1-C6 113.42(9), O1-P1-O2 117.18(11), O1-P1-O3 114.64(11), O2-P1-C6 101.16(10), O2-P2-O3 102.75(9), O3-P1-C6 106.10(9), C2-Br1-O1 A 165.04(10). Torsion angles (°): O1-P1-C6-C5 11.4(2), O1-P1-C6- N1 169.57(18). Symmetry codes: [A] 1 + x, y, 1 + z; [B] −1 + x, y, −1 + z; [C] 2 + x, y, 2 + .

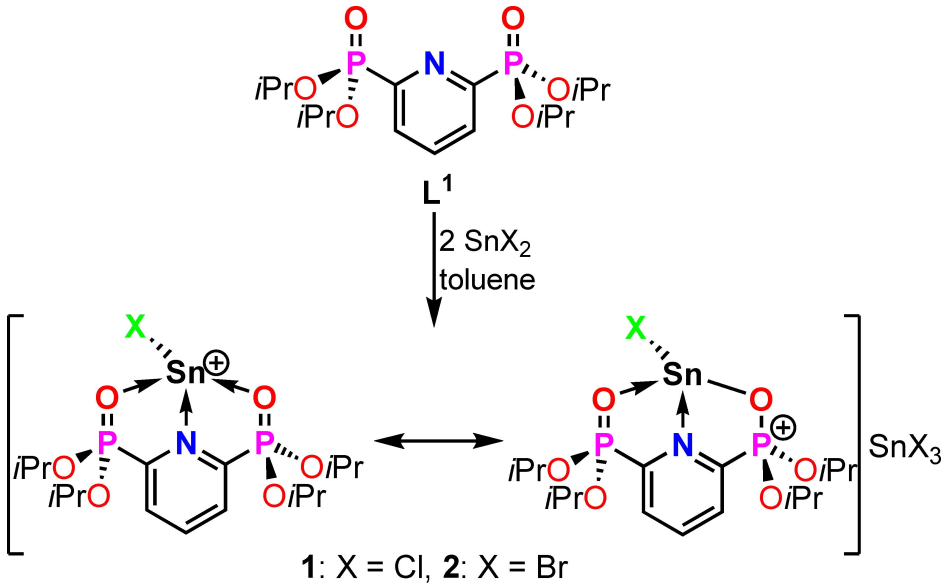

Scheme 3. Synthesis of the complexes **1** and **2.**

crystalized as its toluene solvate **1**·C_7H_8 in the triclinic space group $P\bar{1}$ with two ion pairs in the unit cell. Figures 2–4 show the molecular structures of **1**, **1**·C_7H_8, and **2**, respectively, including the connectivity patterns induced by intermolecular chlorine (for **1**, **1**·C_7H_8) and bromine (for **2**) bridges. The figure captions contain selected interatomic distances and angles.

Considering the lone electron pair at Sn1 being stereochemically active and all the interatomic Sn1-Cl, Sn1-Br, Sn1-N, and Sn1-O distances given in the captions of Figures 2 and 4, and being shorter than the sums of the van der Waals radii[12a–c] of these atoms (SnCl 3.92, SnBr 4.00, SnN 3.72, SnO 3.69 Å), the Sn1 centre in **1** can be seen with caution as pseudo eight-coordinate, and the Sn1 in both **1**·C_7H_8 and **2** as pseudo seven-coordinate with the last two in strongly distorted pentagonal bipyramidal environments. In these, the N1, O1, O4, O4B, and the lone electron pair (in **1**·C_7H_8) and N1, O1, O4, Br1 A, and the lone electron pair (in **2**) occupy the equatorial positions while the Cl1 and Cl2 (in **1**·C_7H_8) and the Br1 and Br2 (in **2**) occupy the axial positions. One way to rationalize the coordination environment about Sn1 is to see it as a bicapped pseudo octahedron in which Cl3 A and Cl4 A approach the Sn1 via the trigonal faces defined by O1, Cl1, lone electron pair and O4, Cl1, lone electron pair, respectively. Figure 5 illustrates these coordination environments. The intramolecular Sn1-O distances are similar and vary between 2.3535(14) (Sn1-O1 in **1**·C_7H_8) and 2.399(4) Å (Sn1-O4 in **1**). The Sn1-N1distances vary between 2.4261(16) (**1**·C_7H_8)

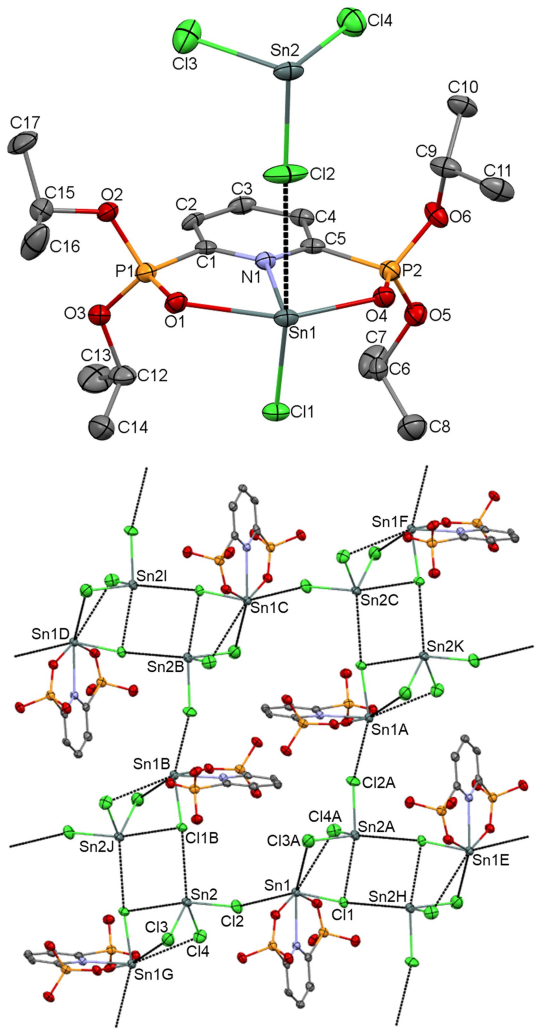

Figure 2. Molecular structure (upper part) and intermolecular connectivity (lower part) of compound **1** (ORTEP presentations at 50% probability of the depicted atoms and atom numbering scheme). The hydrogen atoms in the upper part and the hydrogen atoms and *i*-propyl substituents in the lower part have been omitted. Selected interatomic distances (Å): Sn1-Cl1 2.4958(14), Sn1-Cl2 3.1538(17), Sn1-Cl3 A 3.7042(19), Sn1-Cl4 A 3.4658(17), Sn1-O1 2.375(4), Sn1-O4 2.399(4), Sn1-N1 2.526(4), Sn2-Cl2 2.5540(16), Sn2-Cl3 2.4681(17), Sn2-Cl4 2.4968(16), Cl1-Sn2 A 3.2708(14), Sn2-Cl1B 3.6198(14), P1-O1 1.470(4), P2-O4 1.476(4). Selected interatomic angles (°): Cl1-Sn1-Cl2 156.62(4), C1-P1-O1 108.6(2), P1-O1-Sn1 125.3(2), O1-Sn1-O4 140.84(12), Sn1-O4-P2 125.0(2), O4-P2-C5 107.8(2), P2-C5-N1 115.2(4), C5-N1-C1 117.9(4), N1-C1-P1 114.7(4), C3-N1-Sn1 176.4(1). Symmetry codes: [A] $^1/_2-x, -^1/_2+y, z$; [B] $-^1/_2+x, ^1/_2-y, 1-z$; [C] $-x, -y, 1-z$; [D] $-1+x, y, z$; [E] $1-x, -y, 1-z$; [F] $-^1/_2+x, -^1/_2-y, 1-z$; [G] $^1/_2-x, ^1/_2+y, z$; [H] $^1/_2+x, ^1/_2-y, 1-z$; [I] $-^1/_2-x, -^1/_2+y, z$; [J] $-x, 1-y, 1-z$; [K] $x, -1+y, z$.

and 2.526(4) (**1**). In fact, the bigger distances in **1** support the interpretation of Sn1 having a high coordination number (vide supra).

Despite the fact that **1** and its toluene solvate **1**·C_7H_8 show similar interatomic distances and angles, their crystal structures differ (Figures 2, 3). In **1**, there are additional intermolecular Sn1-Cl3 A, Sn1-Cl4 A, Cl1-Sn2 A, and Cl1-Sn2H interactions at distances of 3.7042(19), 3.4658(17), 3.2708, and 3.620(2) Å, respectively, linking two $[L^1Sn1Cl1]^+$ cations centrosymmetric. In **1**·C_7H_8, the $[L^1SnCl]SnCl_3$ units are alternatingly linked via Sn2-Cl3A–Sn2A and Sn1-O4B–Sn1B bridges at Sn2-Cl3 A and Sn1-O4B distances of 3.5845(6) and 3.1015(16) Å, respectively, giving an infinitive chain (Figure 3). The disordered toluene molecules occupy the space between the chains (see Supporting Information, Figure S1). In the crystal structure of **2** (Figure 4) the $[L^1SnBr]SnBr_3$ forms a head-to-head centrosymmetric dimer via unsymmetrical Sn1-Br1-Sn1 A/Sn1-Br1A–Sn1A bridge [Sn1-Br1 2.6476(3) Å, Sn1-Br1A 3.745(3) Å]. The two terminal $[SnBr_3]^-$ anions (containing Sn2 and Sn2A) of this dimer link it to symmetry-related dimers giving a two-dimensional honey comb-like network. The Sn2 centre is pseudo hexacoordinate by Br2, Br3, Br4, Br3D, Br4D and the lone electron pair at Sn–Br distances ranging in between 2.6447(3) (Sn2-Br4) and 3.862(3) Å (Sn2-Br4D).

Exemplarily, a ^{1}H NMR spectrum of a solution of compound **1** in CD_2Cl_2 shows the signal for the *para* (δ 8.63 ppm) and *meta* (δ 8.30 ppm) protons of the pyridine moiety shifted downfield in comparison to the corresponding signals of the free ligand $\mathbf{L^1}$ (δ 7.91, 7.81 ppm). The *CH*Me$_2$ protons appear as complex pattern centred at δ 5.07 ppm and the *CH*$_3$ protons show two equally intense doublet resonances at δ 1.31 [$^3J(^1H–C–C–^1H)$ 6 Hz] and δ 1.49 ppm [$^3J(^1H–C–C–^1H)$ 6 Hz], respectively. A ^{13}C NMR spectrum of the same solution reveals for the *CH*$_3$ carbon atoms two doublet resonances at δ 24.0 [$^3J(^{13}C–^{31}P)$ 3 Hz] and 23.9 ppm [$^3J(^{13}C–^{31}P)$ 5 Hz], and a doublet for the *CH* carbon atoms at δ 77.2 [$^2J(^{13}C-^{31}P)$ 6 Hz]. A doublet of doublet resonance at δ 147.8 ppm [$^1J(^{13}C–^{31}P)$ 217 Hz, $^3J(^{13}C–^{31}P)$ 18 Hz] belongs to C_i, while the doublet of doublet resonance at δ 132.8 ppm [$^2J(^{13}C–^{31}P)$ 19 Hz, $^4J(^{13}C–^{31}P)$ 3 Hz] is assigned to C_o. The C_p carbon atom shows a triplet resonance at δ 143.0 ppm [$^3J(^{13}C–^{31}P)$ 9 Hz]. The $^{31}P\{^1H\}$ NMR spectra of **1** and **2** display singlet resonances at δ 17.9 (**1**) and δ 16.3 (**2**) ppm being downfield shifted compared to free $\mathbf{L^1}$ (δ 7.9 ppm). No $^{119}Sn\{^1H\}$ NMR resonance was observed at 298 K, apparently indicating kinetic lability of the P=O→Sn and N→Sn interactions on the ^{119}Sn NMR time scale. However, a $^{119}Sn\{^1H\}$ NMR spectrum of a CD_2Cl_2 solution of compound **1** at 193 K revealed two equally intense resonances at δ −90 (*Sn*Cl_3^-) and δ −701 ppm (L^1*Sn*Cl^+). These signals are high field shifted as compared to the related tin complexes [2,6-{C(CH$_3$)=N(C$_6$H$_3$-2,6-*i*-Pr$_2$)}2-C$_6$H$_3$NSnCl]SnCl$_3$ (δ^{119}Sn −60 and −435 ppm)[6a] and [2-{C(CH$_3$)=N(C$_6$H$_3$-2,6-*i*-Pr$_2$)}-6-(OCH$_3$)-C$_6$H$_3$NSnCl]SnCl$_3$ (δ^{119}Sn −73 and −330 ppm).[7]

The reaction of the unsymmetrically substituted pyridine phosphonate 2-{(*i*-PrO)Ph(O)P}-6-{(*i*-PrO)$_2$(O)P}C$_5$H$_3$N ($\mathbf{L^2}$) with two molar equivalents $SnCl_2$ furnished the complex $[L^2SnCl]SnCl_3$ (**3**), containing two stereogenic centres (Scheme 4).

It was obtained as colourless solid material, showing a good solubility in toluene, acetonitrile and THF. Slow evaporation of its saturated toluene solution provided single crystals suitable for X-ray diffraction analysis. Figure 6 shows the molecular structure and the intermolecular connectivity in the crystal by C–H···O interactions. The figure caption contains selected interatomic distances and angles.

Compound **3** crystallized in the monoclinic space group *Pc* containing two ion pairs in the unit cell. Both Sn1 and P1 are stereogenic centres. Consequently, the two cations in the unit

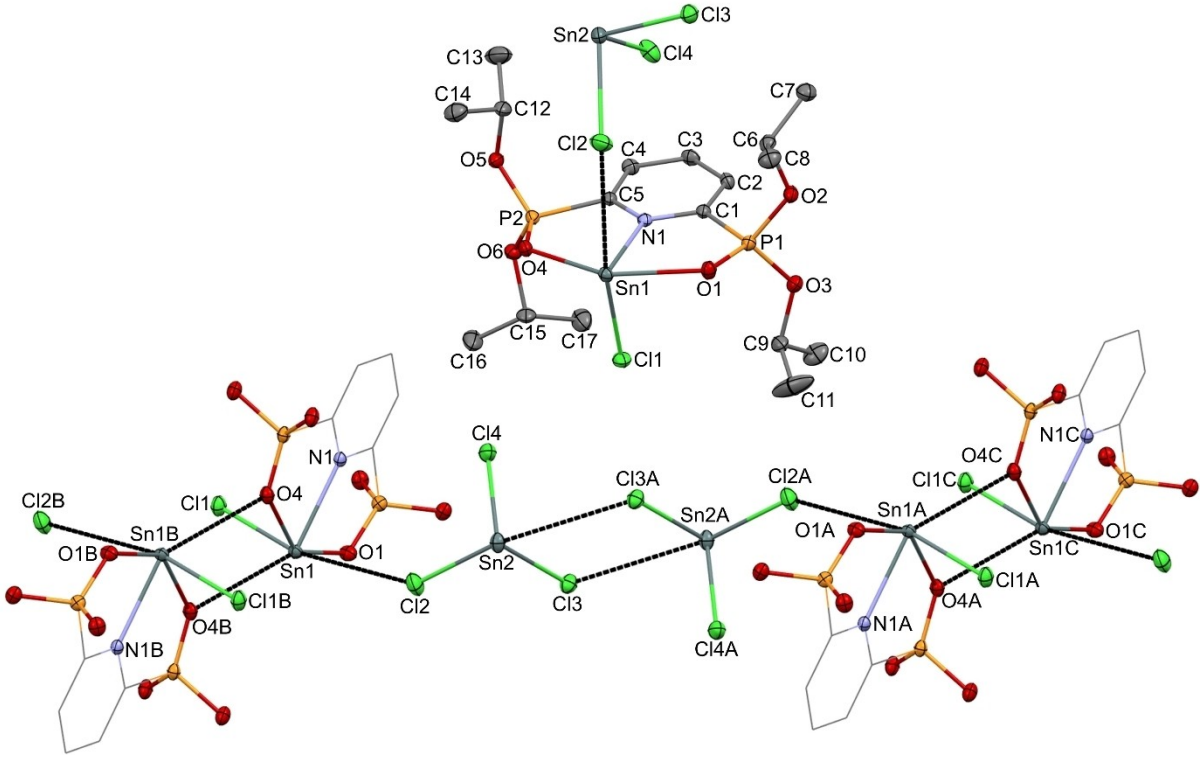

Figure 3. Molecular structure (upper part) and intermolecular connectivity (lower part) of compound **1**·C_7H_8 (ORTEP presentations at 50% probability of the depicted atoms and atom numbering scheme). The toluene solvate molecule, the hydrogen atoms (upper part), and the hydrogen atoms and the *i*-propyl substituents in the lower part have been omitted for clarity. Selected interatomic distances (Å): Sn1-Cl1 2.4646(5), Sn1-Cl2 3.3071(6), Sn1-O1 2.3535(14), Sn1-O4 2.3760(14), Sn1-O4B 3.1015(16), Sn1-N1 2.4261(16), P1-O1 1.4802(15), P2-O4 1.4834(15), Sn2-Cl2 2.4858(6), Sn2-Cl3 2.4670(5), Sn2-Cl4 2.4644(6), Sn2-Cl3 A 3.5845(6). Selected interatomic angles (°): Cl1-Sn1-Cl2 166.08(2), Cl2-Sn2-Cl3 A 166.35(2), C1-P1-O1 106.80(9), P1-O1-Sn1 123.90(8), O1-Sn1-O4 144.89(5), Sn1-O4-P2 123.40(8), O4-P2-C5 106.89(9), P2-C5-N1 115.71(14), C5-N1-C1 118.09(17), N1-C1-P1 116.08(15), C3-N1-Sn1 179.5 (1). Symmetry codes: [A] 2−x, 1−y, 1−z; [B] 1−x, 1−y, 2−z; [C] 1+x, y, −1+z.

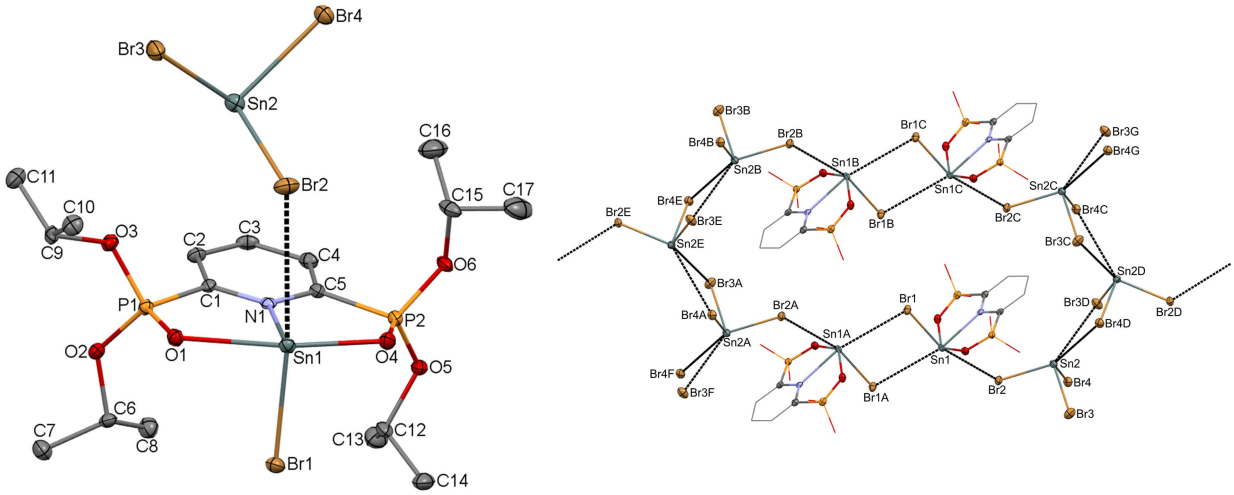

Figure 4. Molecular structure (left) and intermolecular connectivity (right) of compound **2** (ORTEP presentations at 50% probability of the depicted atoms and atom numbering scheme). The hydrogen atoms in the upper part and the hydrogen atoms and *i*-propyl substituents in the lower part have been omitted. Selected interatomic distances (Å): Sn1-Br1 2.6476(3), Sn1-Br(2) 3.319(3), Sn1-Br1 A 3.745(3), Sn1-O1 2.3574(17), Sn1-O4 2.3731(18), Sn1-N1 2.458(2), Sn2-Br2 2.6991(3), Sn2-Br3 2.6480(3), Sn2-Br4 2.6447(3), Sn2-Br3D 3.605(3), Sn2-Br4D 3.862(3), P1-O1 1.4828(18), P2-O4 1.4801(19). Selected interatomic angles (°): Br1-Sn1-Br2 163.08(1), N1-Sn1-Br1 A 163.76(5), C1-P1-O1 108.53(11), P1-O1-Sn1 123.01(10), O1-Sn1-O4 143.26(6), Sn1-O4-P2 124.19(10), O4-P2-C5 107.08(11), P2-C5-N1 115.30(19), C5-N1-C1 117.9(2), C3-N1-Sn1 173.9(1). Symmetry codes: [A] 1−x, 1−y, 1−z; [B] 1−x, −y,1−z; [C] x, −1+y, z; [D] ½ −x, −½ +y, ½−z; [E] ½+x, ½−y, ½+z; [F] ½+x, 1½−y, ½+z; [G] ½−x, −1½+y, ½−z.

cell are diastereomers existing as pair of enantiomers P(*R*)Sn(*S*)/P(*S*)Sn(*R*). The Sn(1) centre is coordinated by N1, O1, O4, Cl1, and Cl2 in a distorted *pseudo* octahedral environment with O1 and O4, and Cl1 and Cl2 being trans with angles of 146.0(3) and

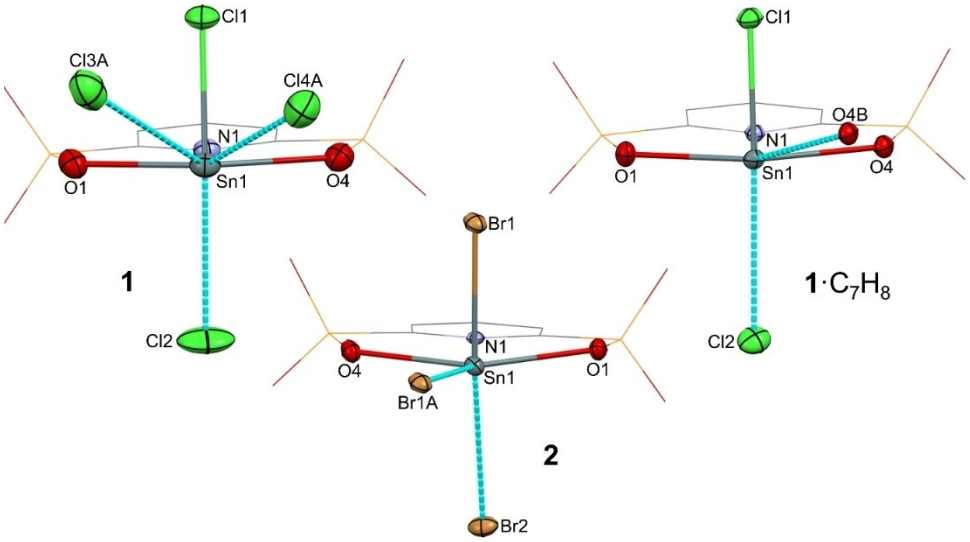

Figure 5. Simplified/reduced presentation of the coordination environment about the Sn1 centres in the compounds **1**, **1**·C_7H_8, and **2** considering the Sn-halogen, Sn–O, and Sn–N distances being shorter than the sums of the van der Waals radii[12a–c] of the atoms involved. The *i*-propyl substituents and the hydrogen atoms have been omitted for clarity.

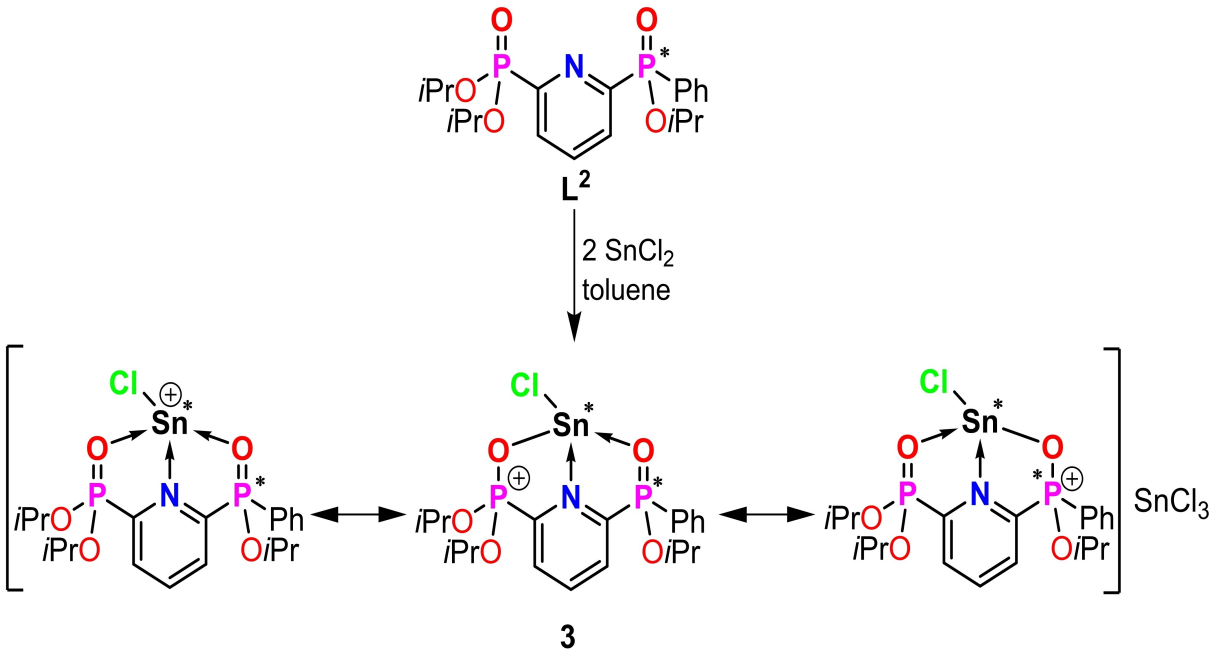

Scheme 4. Synthesis of [L^2SnCl]$SnCl_3$ (**3**).

157.00(3)°, respectively. The N1 is trans to the lone electron pair at Sn1.

The structure resembles that of the complex **1** with the essential difference that in **3** the Sn1—O4 distance of 2.295(9) Å is much shorter than the Sn1—O1 distance of 2.406(8) Å. This indicates a superior donor capacity of the PhP(O)(O*i*Pr) versus the P(O)(O*i*Pr)$_2$ moiety, as it was also reported by Weichmann et al. for 2,2-functionally disubstituted triorganotin chlorides.[13] An interesting aspect in the structure of **3** is the σ-π interaction between Sn2 and the phenyl ring with distances to the carbon atoms C(18), C(19) and C(20) of 3.7928(90), 3.6629(85), and 3.7348(75) Å, respectively, being slightly shorter than the sum of the van der Waals radii (3.87 Å)[12a–c] of the atoms involved. In the crystal, **3** forms an infinite chain by a H2···O4 contact at a distance of 2.5011(13) Å (C2···O4 3.371(1) Å). The chains are connected by intermolecular Sn2···Cl1 interactions at a distance of 3.7625(34) Å.

A ^{1}H NMR spectrum (400.25 MHz, 298 K) of a solution of **3** in CD_2Cl_2 show complex resonances for the *o*-, *m*, and *p*-protons of the phenyl substituent centred at δ 8.15, 8.27, and 8.60 ppm, respectively. The pyridine protons appear at δ 7.74 (H_p) and 7.64 (H_m) ppm. The resonances for the different OC*H* protons

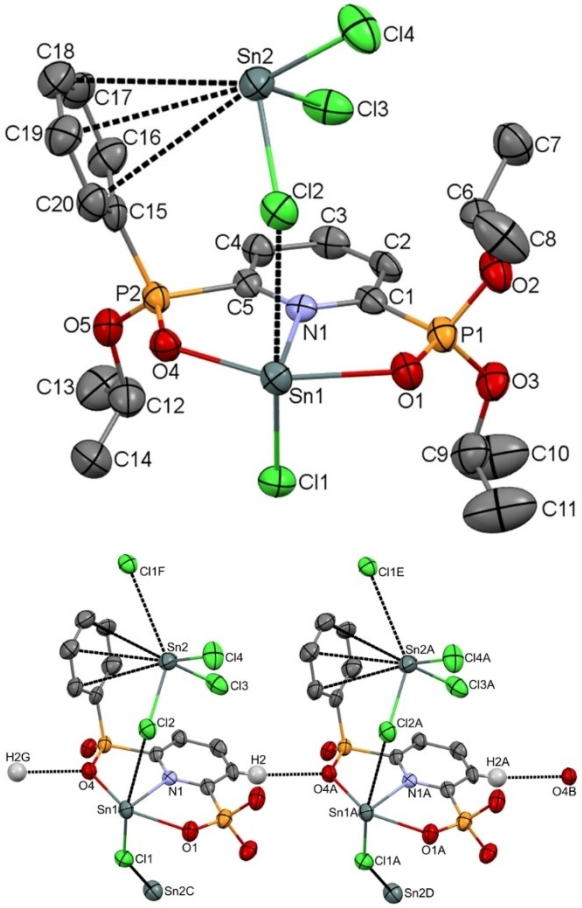

Figure 6. Molecular structure (upper part) and intermolecular connectivity (lower part) of compound **3** (ORTEP presentations at 50% probability of the depicted atoms and atom numbering scheme). With exception of H2, the hydrogen atoms have been omitted for clarity. Selected interatomic distances (Å): Sn1-Cl1 2.4780(31), Sn1-Cl2 3.2154(35), Sn1-N1 2.4045(91), Sn1-O1 2.406(8), Sn1-O4 2.295(9), Sn2-Cl2 2.529(4), Sn2-Cl3 2.454(4), Sn2-Cl4 2.455(4), Sn2-Cl1F 3.7625(34), P1-O1 1.468(5), P1-O2 1.558(6), P1-O3 1.554(6), P2-O4 1.489(6), P2-O5 1.553(6), H(2)-O(4 A) 2.5011(13) Å. Selected interatomic angles (°): Cl1-Sn1-Cl2 157.0(1), N1-Sn1-Cl1 82.6(2), C1-P1-O1 107.1(5), P1-O1-Sn1 122.4(5), O1-Sn1-O4 146.0(3), Sn1-O4-P2 124.4(5), O4-P2-C5 105.9(5), P2-C5-N1 115.1(8), C5-N1-C1 118.8(9), N1-C1-P1 117.5(6), C3-N1-Sn1 173.4(1). Symmetry codes: [A] 1+x, y, z; [B] 2+x, y, z; [C] x; 1−y, $^1/_2$ +z; [D] 1+x, 1−y, $-^1/_2$ +z; [E] 1+x, 1−y, $^1/_2$ +z; [F] x, 1−y, $^1/_2$ +z; [G] −1+x, y, z.

are superimposed and show a complex pattern centred at δ 5.07 ppm. The coupling patterns of these resonances were not analysed in detail. The CH_3 protons show six doublet resonances at δ 1.52, 1.50, 1.46, 1.37, 1.33 and 1.27 ppm, respectively, with $^3J(^1H–C–C–^1H)$ of 6 Hz. A $^{31}P\{^1H\}$ NMR spectrum of the same sample at room temperature displayed two equally intense singlet resonances at δ 36.7 and 15.8 ppm, respectively, which are shifted downfield as compared to the respective signals of free **L²** (δ 22.3 and 7.2 ppm). At 193 K, de-coalescence of the resonance at 35.8 ppm into two almost equally intense signals at δ 37.4 and 36.7 ppm takes place while the signal at 15.8 ppm shifted slightly to δ 17.0 ppm but remained sharp. A ^{119}Sn NMR spectrum at room temperature did not reveal any signal, but at 193 K three resonances at δ −89, −673, and −681 ppm were observed. The results are interpreted in terms of compound **3** existing as two diastereomers the epimerization of which is fast at room temperature but slow at 193 K on the corresponding NMR time scales.

Synthesis and Structures of the Carbmethoxylate- and Carbamide-containing tin(II) Complexes 4 and 5, and 6 and 7, respectively

Similar to the syntheses of compounds **1**–**3**, the reaction of 2,6-$[MeO(O)C]_2C_5H_3N$ (**L³**) and 2,6-$[Et_2N(O)C]_2C_5H_3N$ (**L⁴**), respectively, with the corresponding tin(II) halides in toluene at room temperature provided the novel tin(II) salts **4**–**7** of types $[L^3SnX]SnX_3$ (**4**, X=Cl; **5**, X=Br) and $[L^4SnX]SnX_3$ (**6**, X=Cl; **7**, X=Br) (Scheme 5).

The compounds **4**–**7** were isolated as pale-yellow solid materials showing good solubility in common polar solvents such as methanol, acetonitrile and THF. Single crystals suitable for X-ray diffraction analysis of **4**, and of the acetonitrile solvates **4**·CH_3CN and **5**·CH_3CN were obtained by storage of their saturated acetonitrile solutions at room temperature. Single crystals of **6** and **7** were grown by slow evaporation of their methanol solutions. The Figures 7–11 show the molecular structures, the intermolecular connectivity in the crystals, and the corresponding figure captions contain selected interatomic distances and angles. Figure 12 illustrates in a simplified manner the coordination environment about the Sn1 centres in these compounds.

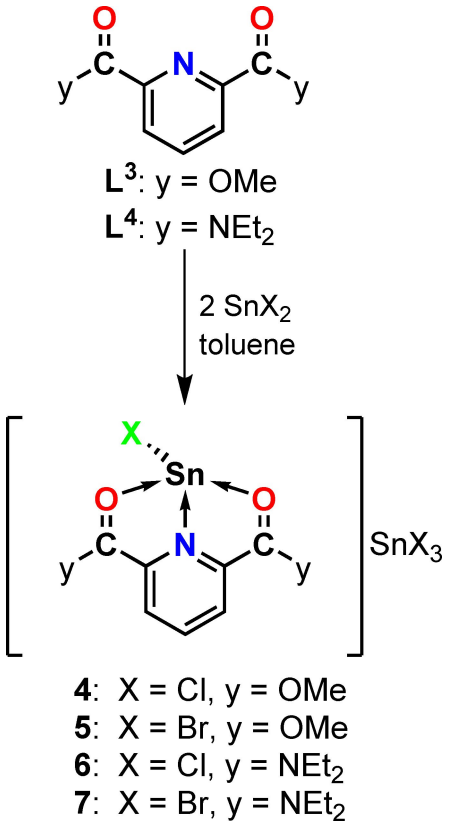

Scheme 5. Syntheses of the tin salts **4**–**7**.

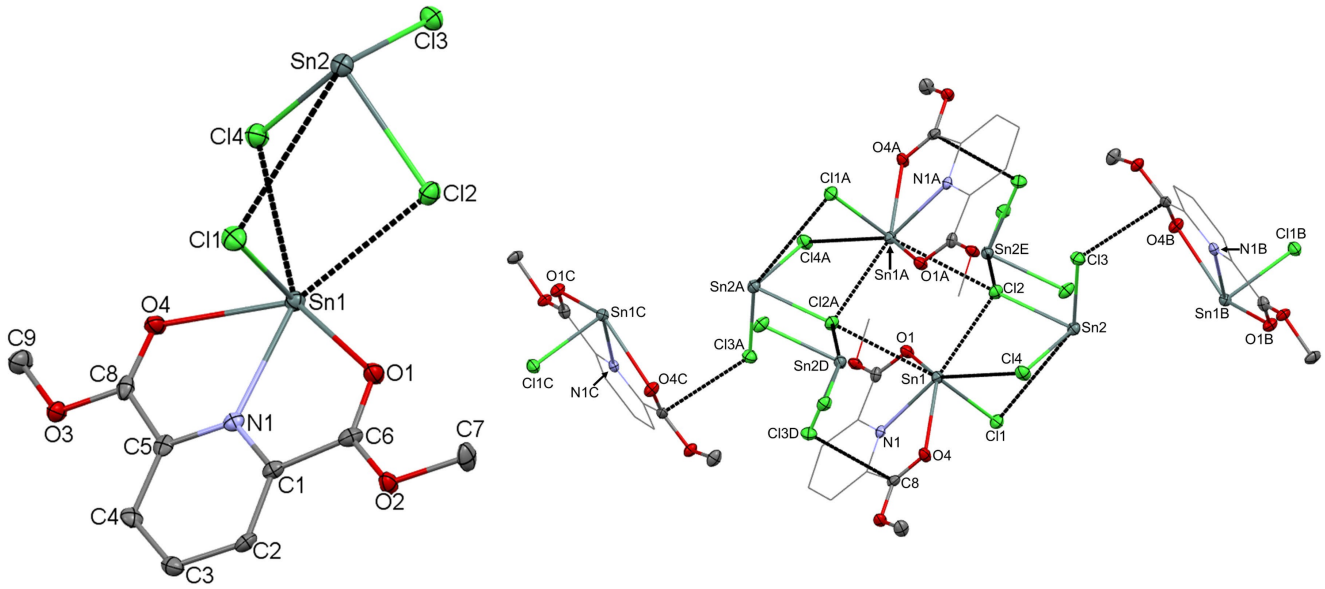

Figure 7. Molecular structure (left) and intermolecular connectivity (right) of compound **4** (ORTEP presentations at 50% probability of the depicted atoms and atom numbering scheme). The hydrogen atoms have been omitted for clarity. Selected interatomic distances (Å): Sn1-Cl1 2.4799(9), Sn1-Cl2 2.994(1), Sn1-Cl4 3.151(1), Sn1-Cl2 A 3.391(1), Sn1-O1 2.478(3), Sn1-O4 2.554(2), Sn1-N1 2.460(3), O1-C6 1.221(4), O2-C6 1.314(4), O3-C8 1.318(4), O4-C8 1.217(4), Cl3D–C8 3.102(3), Sn2-Cl2 2.6517(9), Sn2-Cl3 2.4596(9), Sn2-Cl4 2.4851(9), Sn2-Cl1 3.8363(10). Selected interatomic angles (°): Cl1-Sn1-Cl2 85.52(3), Cl1-Sn1-Cl4 80.69(3), N1-Sn1-Cl2 141.68(7), N1-Sn1-Cl4 142.74(7) C1-C6-O1 122.0(3), C1-C6-O2 113.1(3), O1-C6-O2 124.9(3), C6-O1-Sn1 118.7(2), O1-Sn1-O4 129.88(8), Sn1-O4-C8 117.5(2), O3-C8-C5 112.5(3), O4-C8-C5 122.5(3), O3-C8-O4 125.0(4), C8-C5-N1 113.5(3), C5-N1-C1 118.2(3), N1-C1-C6 113.0(3), C3-N1-Sn1 173.7(1). Symmetry codes: [A] 1−x, 1−y, 1−z; [B] ½+x, 1½−y, 1−z, [C] ½−x, −½+y, z; [D] −½+x, 1½−y, 1−z; [E] 1½−x, −½+y, z.

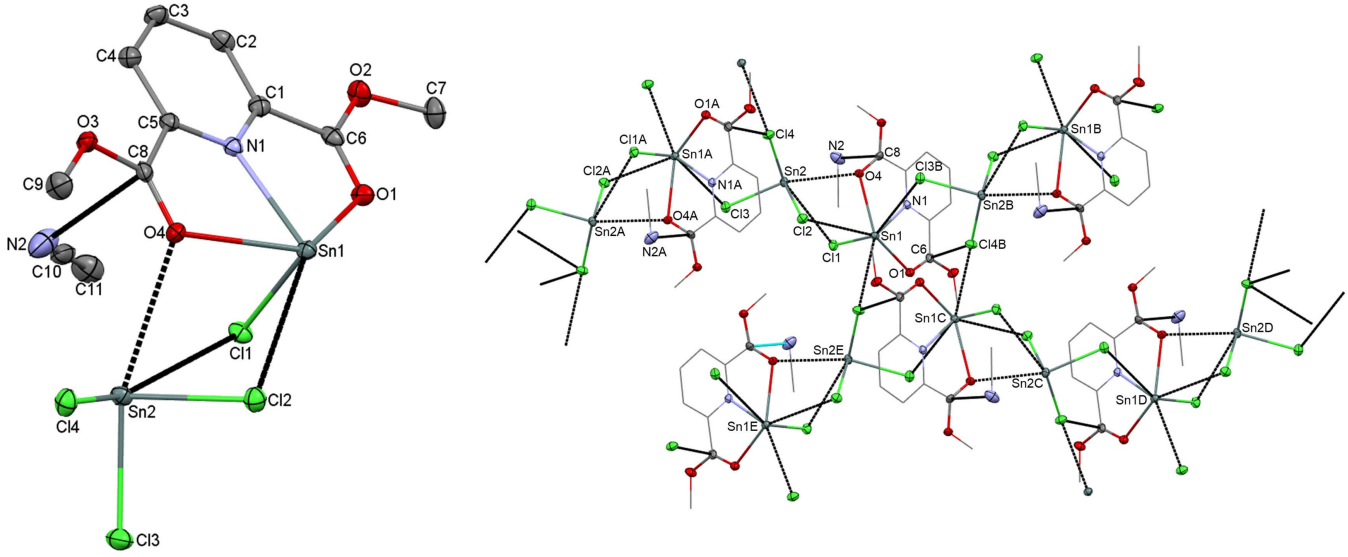

Figure 8. Molecular structure (left) and intermolecular connectivity (right) of compound **4**·CH_3CN (ORTEP presentations at 50% probability of the depicted atoms and atom numbering scheme). The hydrogen atoms have been omitted for clarity. Selected interatomic distances (Å): Sn1-Cl1 2.4775(11), Sn1-Cl2 3.275(11), Sn1-Cl3B 3.521(11), Sn1-Cl4E 3.172(11), Sn1-O1 2.489(2), Sn1-O4 2.545(2), Sn1-N1 2.392(2), O1-C6 1.227(3), O2-C6 1.316(3), O3-C8 1.314(3), O4-C8 1.219(3), N2-C8 3.086(2), Cl4B–C6 3.122(2), Sn2-Cl1 3.454(11), Sn2-Cl2 2.4993(11), Sn2-Cl3 2.5158(13), Sn2-Cl4 2.5320(11), Sn2-O4 3.004(2). Selected interatomic angles (°): O1-Sn1-O4 131.56(6), O1-Sn1-Cl1 81.26(6), O1-Sn1-Cl2 150.17(6), O1-Sn1-N1 66.76(7), N1-Sn1-Cl1 86.23(7), N1-Sn1-Cl2 130.96(7), Cl1-Sn1-Cl2 77.05(6), Cl3-Sn2-O4 162.16(6), N2-C8-C5 81.71(6), N2-C8-O3 95.21(6), N2-C8-O4 92.64(6), O3-C8-O4 125.8(3), O3-C8-C5 112.3(2), O4-C8-C5 121.9(2), O1-C6-O2 125.3(3), O1-C6-C1 122.1(3), O2-C6-C1 112.7(2). Symmetry codes: [A] 2−x, ½+y, ½−z; [B] 2−x, −½+y, ½−z; [C] 2−x, 1−y, 1−z; [D] x, ½−y, ½+z; [E] x, 1.5−y, ½+z.

Compound **4** crystallized in the orthorhombic space group *P*bca with eight ion pairs per unit cell. The Sn1 cation is coordinated by N1, O1, O4, and Cl1 at distances of 2.460(3), 2.478(3), 2.554(3), and 2.4799(9) Å, respectively. In addition, there are weak Sn1−Cl2 (2.994(3) Å), Sn1−Cl4 (3.151(3) Å) and Sn1−Cl2 A (3.391(3) Å) interactions giving, under participation of its lone electron pair, the Sn(1) a *pseudo*-eightfold coordination (Figures 7, 12). The Sn(2) centre is four-coordinate by the chlorine atoms Cl1-Cl4 at distances ranging between 2.4596(9) (Sn2-Cl3) and 3.8363(10) Å (Sn2-Cl1) with the latter being only

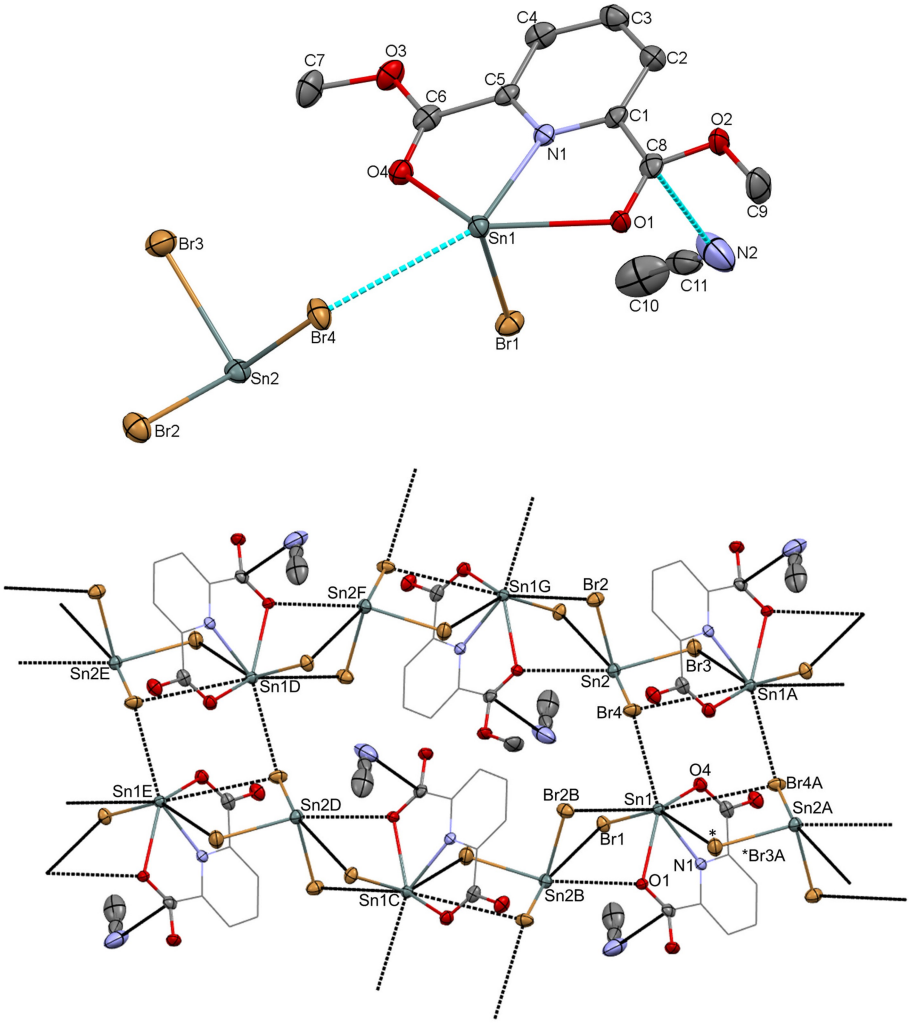

Figure 9. Molecular structure (upper part) and intermolecular connectivity (lower part) of compound **5**·CH_3CN (ORTEP presentations at 50% probability of the depicted atoms and atom numbering scheme). The hydrogen atoms have been omitted for clarity. Selected interatomic distances (Å): Sn1-Br1 2.6330(6), Sn1-Br4 3.2478(5), Sn1-Br2B 3.4328(6), Sn1-Br3 A 3.7211(6), Sn1-Br4 A 3.8234(6), Sn1-O1 2.548(3), Sn1-O4 2.478(3), Sn1-N1 2.397(3), O1-C8 1.219(5), O1-Sn2B 3.0718(30), O2-C8 1.321(5), O3-C6 1.313(5), O4-C6 1.222(5), N2-C8 3.0863(72). Selected interatomic angles (°): Br1-Sn1-Br4 86.8(2) Br1-Sn1-Br4 A 138.0(1), C1-C8-O1 122.5(4), C1-C8-O2 112.3(4), O1-C8-O2 125.2(4), C8-O1-Sn1 114.6(3), O1-Sn1- O4 130.96(10), Sn1-O4-C6 116.6(3), O3-C6-C5 112.7(4), O4-C6-C5 122.0(4), O3-C6-O4 125.3(4), C6-C5-N1 113.4(4), C5-N1-C1 118.5(4), C3-N1-Sn1 173.7(1), N1-C1-C8 113.5(4), N1-Sn1-Br4 143.4(1). Symmetry codes: [A] −x, 1−y, 1−z; [B] x, $^1/_2$−y, $^1/_2$+z; [C] −x, $^1/_2$+y, $1^1/_2$−z; [D] −x, −y, 1−z; [E] x, −1+y, z; [F] −x, $-^1/_2$+y, $^1/_2$−z; [G] x, $^1/_2$−y, $-^1/_2$+z.

slightly shorter than the sum of the van der Waals radii[12a–c] of these atoms (vide supra). Considering participation of the lone electron pair, the Sn2 adopts a *pseudo* trigonal bipyramidal environment.

In the crystal structure, two [L^3SnCl]$SnCl_3$ moieties form a centrosymmetric dimer via intermolecular Sn1-Cl2 and Sn1-Cl2 A at distances as mentioned above. Notably, there is an intermolecular Cl3D···C8 interaction (Figure 7) at a distance of 3.102(3) Å. This distance is shorter than the sum (3.45 Å) of the van der Waals radii[12a–c] of the atoms involved. The interaction is exclusively electrostatic as it has no significant effect on the angles about C8. The O3-C8-O4 [124.97(1)°], O3-C8-C5 [122.51(1)°], O4-C8-C5 [112.51(1)°] and C1-C6-O1 [122.09(1)], C1-C6-O2 [113.06(1)], and O1-C6-O2 [124.84(1)] angles differ only negligible.

The acetonitrile solvate **4**·CH_3CN crystallized in the monoclinic space group $P2_1/c$ with four ion pairs [L^3SnCl]$SnCl_3$ in the unit cell. Indeed, the solvate molecule influences the coordination pattern of the ion pair. Whereas in **4** the $[L_3SnCl]^+$ cation and the $SnCl_3^-$ anion are linked by three Sn–Cl···Sn bridges, in **4**·CH_3CN there are two such bridges (Sn1-Cl1···Sn2, Sn1···Cl2-Sn2) plus a Sn1-O4···Sn2 bridge at Sn1-Cl2, Sn2-Cl1, and Sn2-O4 distances of 3.275(11), 3.454(11), and 3.004(2) Å, respectively, all of these being shorter than the sums of the van der Waals radii[12a–c] of the participating atoms. The N2 donor atom of the acetonitrile solvate molecule approaches the C8 atom and the Cl4B the C6 atom at distances of 3.086(2) and 3.122(2) Å, respectively. Both interactions do not disturb the trigonal planar geometry of the corresponding carbon centres indicating these interactions being purely electrostatic.

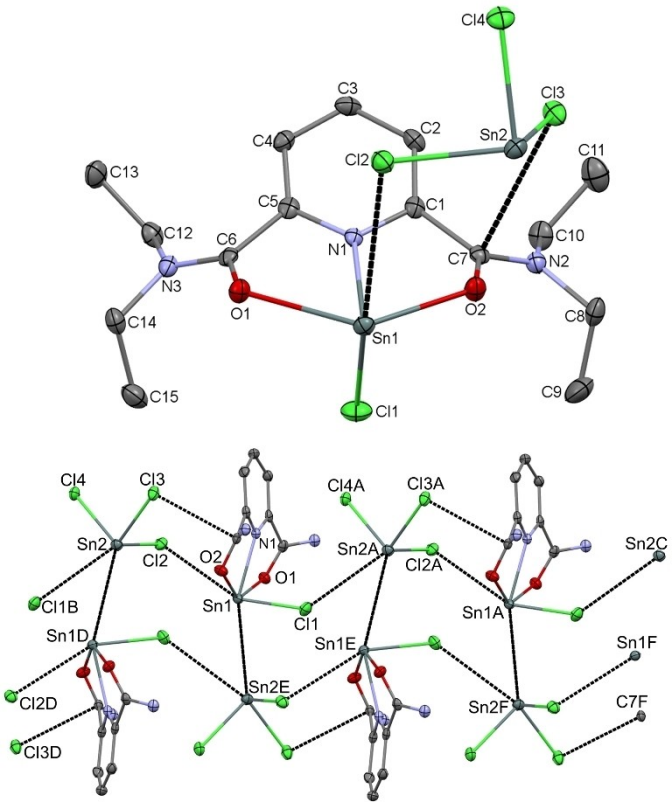

Figure 10. Molecular structure (upper part) and intermolecular connectivity (lower part) of compound **6** (ORTEP presentations at 50% probability of the depicted atoms and atom numbering scheme). The hydrogen atoms have been omitted for clarity. Selected interatomic distances (Å): Sn1-Cl1 2.4738(7), Sn1-Cl2 3.3218(7), Sn1-N1 2.316(2), Sn1-O1 2.2448(18), Sn1-O2 2.4051(17), O1-C6 1.257(3), O2-C7 1.256(3), Cl1-Sn2 A 3.6242(7), Cl3-C7 3.2408(28), N2-C7 1.317(3), N3-C6 1.325(3), Sn1-Sn2E 4.2756(3). Selected interatomic angles (°): Cl1-Sn1-Cl2 153.61(2), Cl1-Sn2A–Cl3A 158.54(2), C1-C7-O2 116.1(2), C7-O2-Sn1 117.59(16), O2-Sn1-O1 136.98(6), Sn1-Cl2-Sn2 106.30(2), Sn1-Cl1-Sn2 A 138.26(2), Sn1-O1-C6 115.41(16), O1-C6-C5 116.4(2), O1-C6-N3 121.7(2), C5-C6-N3 121.8(2), C6-C5-N1 110.0(2), C1-N1-C5 120.2(2), C3-N1-Sn1 162.8 (1), N1-C1-C7 110.0(2), C1-C7-N2 122.9(2), C1-C7-O2 116.1(2), N2-C7-O2 120.9(2), C5-C6-N3 121.8(2), C5-C6-O1 116.4(2), O1-C6-N3 121.7(2). Symmetry codes: [A] x, 1+y, z; [B] x, −1+y, z; [C] x, 2+y, z; [D] 1½−x, −½+y, ½−z; [E] 1½−x, ½+y, ½−z; F 1½−x, 1½+y, ½−z.

A ^{1}H NMR spectrum (400.25 MHz, CD_2Cl_2, 298 K) of **4** shows a singlet resonance for the CH_3 protons at δ 4.02 ppm. The pyridine protons appear as triplet (H_p) and doublet (H_m) resonances at 8.08 and 8.31 ppm, respectively. Compared to the signals observed for the free ligand **L**^{3} [δ 3.98 (CH_3), 8.00 (H_p), (8.25 pm (H_m)], these resonances shifted to lower field as induced by the electron withdrawing Sn^{+} centre.

The analogous bromine derivative **5**·CH_3CN crystallized in the monoclinic space group $P2_1/c$ with four formula units in the unit cell. Again, the Sn1 cation is coordinated by N1, O1, O4, and Br1 at distances of 2.397(3), 2.548(3), 2.478(3), and 2.6330(6) Å, respectively, with the Sn–N1 distance being shorter than the corresponding distance in **4**, and the Sn–O distances differing among each other but being close to those in **4**. In analogy to **4**·CH_3CN (vide supra), the N2 atom of the acetonitrile solvate molecule points to the C8 carbonyl carbon atom at almost the same distance of 3.0863(72) Å. Despite this distance being shorter than the sum of the van der Waals radii[12a–c] of nitrogen (1.55 Å) and carbon (1.70 Å), the interaction does not influence the other distances and angles C8 is involved in. They are within the experimental errors equal to the corresponding values for C6.

The contact of Sn1 to its counter anion $SnBr_3^-$ is realized by a Sn1-Br4 interaction at a distance of 3.2478(5) Å being shorter than the sum of the van der Waals radii[12a–c] (4.00 Å) of the atoms involved. In contrast to the Sn2-bound chlorine atom Cl2 in **4**, the Br2 in **5**·CH_3CN does not interact with Sn1 but, together with Br3 and O1 serve to build the supramolecular crystal structure by intermolecular Br–Sn and O–Sn interactions at distances of 3.4328(6), 3.7211(6), and 3.0718(30), respectively.

Compound **6** containing the carbamide-substituted pyridine ligand **L**^{4} crystallized in the monoclinic space group $P2_1/n$ with four formula units in the unit cell. The N1, O1, O2, Cl1 and Cl2 atoms coordinate the Sn1 centre at interatomic distances of 2.316(2), 2.2448(18), 2.4051(17), 2.4738(7), and 3.3218(7) Å, respectively, giving it a distorted pseudo octahedral coordination environment with Cl1 and Cl2, and O1 and O2 trans, and in which the lone electron pair at Sn1 occupies the position trans to N1. The [L^{4}SnCl]$SnCl_3$ ion pairs form an infinite chain along the y-axis via a weak intermolecular Cl1-Sn2 A interaction at a distance of 3.6242(7) Å being shorter than the sum of the van der Waals radii[12a–c] (3.92 Å) of these atoms. The Sn1 centres of one chain interact with the Sn2 centres of a neighbour chain at a Sn–Sn distance of 4.2756(3) Å which is just below twice the van der Waals radius[12a–c] of Sn (4.34 Å). A second remarkable feature is the Cl3-C7 distance of 3.2408(28) Å being 0.21 Å below the sum of the van der Waals radii[12a–c] of C (1.70 Å) and Cl (1.75 Å). In analogy to the N8-C8 interaction in **5**·CH_3CN, the Cl3-C7 interaction is electrostatic as its influence on the angles about the C7 centre is negligible when compared with the situation about C6 lacking an interaction with a Cl atom.

A ^{1}H NMR spectrum (600.29 MHz, 298 K) of a solution of **6** in CD_3CN showed a triplet resonance at δ 8.56 ppm for the H_p proton and a doublet resonance at δ 8.28 ppm for the H_o protons of the pyridine ring. The NEt_2 protons showed two equal intensity sets of signals at δ 3.81 and 3.72 ppm (NCH_2CH_3), and δ 1.49 and 1.33 ppm, respectively. Compared to the corresponding resonances for the ligand **L**^{4} (7.93, 7.50, 3.50, 3.25, 1.20, 1.08 ppm), these signals shifted downfield. A ^{13}C NMR spectrum (150.94 MHz, CD_3CN) of the same solution indicated the non-equivalence of the ethyl groups as well, showing in addition to the resonances for the carbonyl and pyridine carbon atoms (δ 167.8, 146.8, 144.4, 129.7 ppm), signals at δ 46.4 and 44.8 ppm (NCH_2CH_3), and δ 13.9 and 12.3 ppm (NCH_2CH_3). A ^{119}Sn NMR spectrum (149.26 MHz, CD_3CN, 298 K) revealed two rather broad resonances at −35 ($\nu_{1/2}$ ~6000 Hz) and −523 ($\nu_{1/2}$ ~7000 Hz) ppm, respectively. The latter data indicate **6** at the onset of kinetic lability on the ^{119}Sn NMR time scale.

Compound **7**, the bromine-substituted analogue of **6**, also crystallized in the monoclinic space group $P2_1/n$ with four formula units in the in the unit cell. Its structure resembles that of **6** with the difference that the secondary Sn1-Sn2B interaction of 4.1772(6) Å is shorter than the corresponding distance in **6** (vide supra). However this distance is longer than the secondary

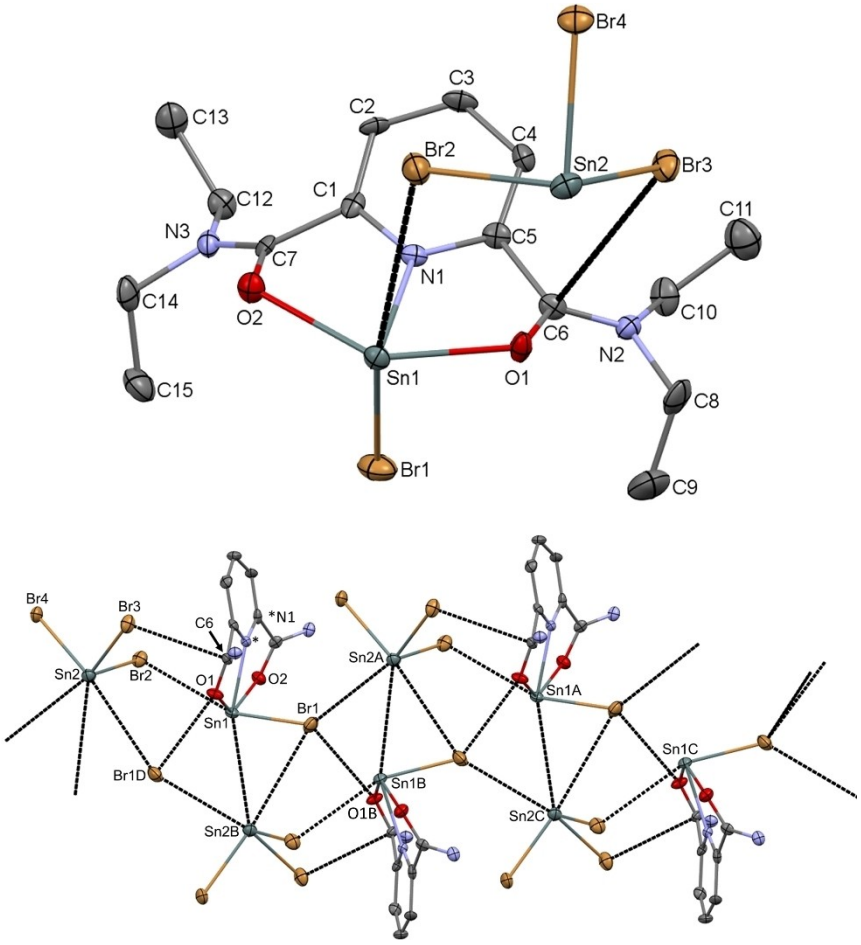

Figure 11. Molecular structure (upper part) and intermolecular connectivity (lower part) of compound **7** (ORTEP presentations at 50% probability of the depicted atoms and atom numbering scheme). The hydrogen atoms have been omitted for clarity. Selected interatomic distances (Å): Sn1-Br1 2.6332(7), Sn1-Br2 3.4083(7), Sn1-O1 2.244(3), Sn1-O2 2.429(3), Sn1-N1 2.321(4), O1-C6 1.249(5), O2-C7 1.266(5), O1-Br1D 3.2734(36), Sn1-Br2 3.4083(7), Br1-Sn2 A 3.6285(7), Br1-Sn2B 3.9848(8), C6-Br3 3.4045(50), Sn1-Sn2B 4.1772(6). Selected interatomic angles (°): Br1-Sn1-Br2 157.11(2), Br1-Sn2A–Br3A 159.61(2), Br1-Sn2B–Br4B 171.87(2), C1-C7-O2 116.1(4), C7- O2-Sn1 115.2(3), O2-Sn1-O1 136.85(11), Sn1-O1- C6 119.3(3), O1-C6-C5 115.4(4), C6-C5- N1 110.5(4), C5-N1-C1 120.3(4), C3-N1-Sn1 160.6(1), N1-C1-C7 110.7(4). Symmetry codes: [A] x, 1 + y, z; [B] 1½ − x, ½ + y, ½ − z; [C] 1½ − x, 1½ + y, ½ − z; [D] 1½ − x, −½ + y, ½ − z.

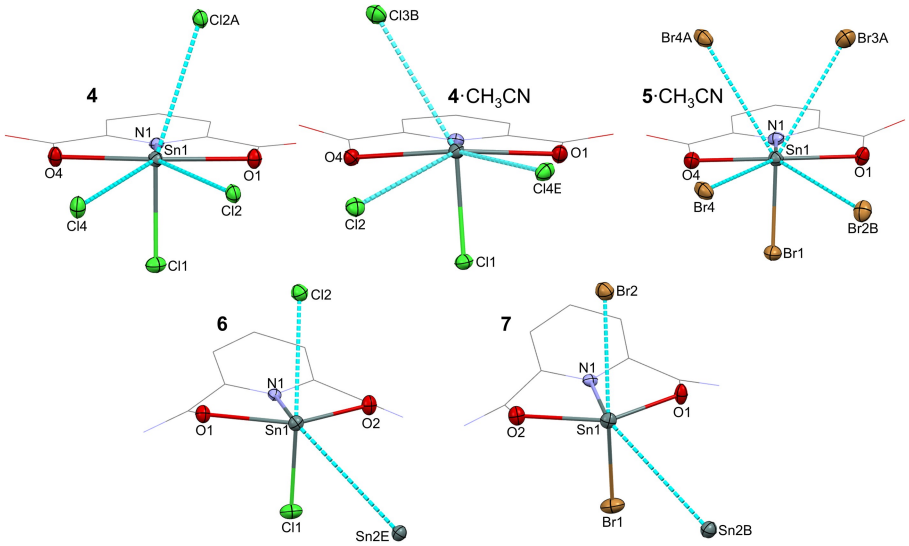

Figure 12. Simplified/reduced presentation of the coordination environment about the Sn1 centres in the compounds **4**, **4**·CH_3CN, **5**·CH_3CN, **6**, and **7** considering the Sn-halogen, Sn–O, Sn–N, and Sn–Sn distances being shorter than the sums of the van der Waals radii[12a–c] of the atoms involved. The methyl (in **4** and **5**·CH_3CN) and ethyl (in **6** and **7**) substituents and the hydrogen atoms have been omitted for clarity, as has been the CH_3CN in **5**·CH_3CN.

Sn–Sn interactions with distances of 3.6809(4), 3.5953(4), 3.8876(3), and 3.8379(5) Å, respectively, observed for [4-*t*Bu-2,6-{P(O)(O*i*Pr)$_2$}$_2$C$_6$H$_2$]SnX (X=Br,[14a] I,[14a] Se,[10] Te[10]).

Thermally Induced Cyclization of the tin(II) Complexes 1, 3, and 4

The thermal stability of the donor-stabilized stannylium trihalogenido stannate salts was exemplarily studied. Thus, heating of toluene solutions of the chlorinated representatives **1** and **3** yielded, via ester cleavage under elimination of 2-chloropropane the novel heterocyclic tin(II) derivatives **8** and **9**, respectively, as solid materials (Scheme 6). Most remarkably, the formation of stereogenic centres at the phosphorus P1 (for **8**), and P1 and P2 (for **9**) and tin atoms (for both **8** and **9**) accompany the cyclization reaction. The Figures 13 and 14 show the molecular structures of **8** and **9**, respectively, the intermolecularconnectivity in the crystals, and the corresponding figure captions contain selected interatomic distances and angles.

Compound **8** crystallized in the triclinic space group $P\bar{1}$with two molecules in the unit cell representing, in analogy as observed for **3** (vide supra), two diastereomers as pair of enantiomers P1(*R*)Sn(*R*)/ P1(*S*)Sn(*S*). The Sn(1) centre is coordinated by N1, O1, O4, Cl1, and Cl2 in a distorted *pseudo* octahedral environment at interatomic distances of 2.4205(17), 2.2647(14), 2.4437(14), 2.5315(6), and 3.1297(6) Å, respectively, and with O1 and O4, and Cl1 and Cl2 being trans with angles of 145.91(5) and 155.30(2)°, respectively. The N1 is trans to the lone electron pair at Sn1. The Cl1 atom coordinates both the Sn2 A and Sn2B centres at distances of 3.1716(5) and 3.631(5) Å which, together with the Sn1-O1B [3.1366(18) Å] create a two-dimensional coordination polymer.

A ^{31}P NMR spectrum of a solution of compound **8** in C_6D_6 at room temperature showed two signals of equal integral at δ 13.4 ($\nu_{1/2}$ ~12 Hz) and 18.9 ($\nu_{1/2}$ ~7 Hz) ppm, respectively. A ^{31}P NMR spectrum at 193 K of **8** dissolved in C_7D_8 revealed two resonances at δ 12.2 [$^2J(^{31}P–O–^{117/119}Sn) = 85$ Hz, unresolved] and 17.8 [$^2J(^{31}P–O-^{117/119}Sn) = 53$ Hz] ppm, respectively. The satellite-to-signal-to-satellite integral ratio of aprox. 1.00:4.62:1.02 for the former signal indicates it to belong to the SnO(*i*PrO)*P*OSnCl$_2$ phosphorus atom which couples with two tin sides. The second resonance belongs to the (*i*PrO)$_2$*P*O phosphorus atom which interacts with one tin side (aprox. satellite-to-signal-to-satellite integral ratio 0.64:5.34:0.63). A ^{119}Sn NMR spectrum (C_6D_6, T = 298 K) showed two resonances at δ −208 and −587 ppm, respectively, and a spectrum of **8** in C_7D_8 at T = 193 K two resonances at δ −267 ($\nu_{1/2}$ ~600 Hz) and −639 ($\nu_{1/2}$ ~500 Hz) ppm, respectively. These data indicate kinetic lability of the P=O→SnCl$_2$ and P=O→SnCl interactions at room temperature on the ^{31}P NMR time scale but kinetic inertness at 193 K.

Compound **9** crystallized in the triclinic space group $P\bar{1}$ as well, with two molecules in the unit cell and, in analogy as observed for **3** and **8** (vide supra), again representing two diastereomers as pair of enantiomers P1(*R*)Sn(*R*)P2(*R*)/ P1(*S*)Sn(*S*)P2(*S*). Unlike in **3** and **8**, in addition to Sn1, both P1 and P2 are stereogenic centres. Consequently, eight diastereomers (as four pairs of enantiomers) should be possible. However, only one pair was isolated as the single crystal actually investigated by X-ray diffraction. The supramolecular structure resembles that of **8**.

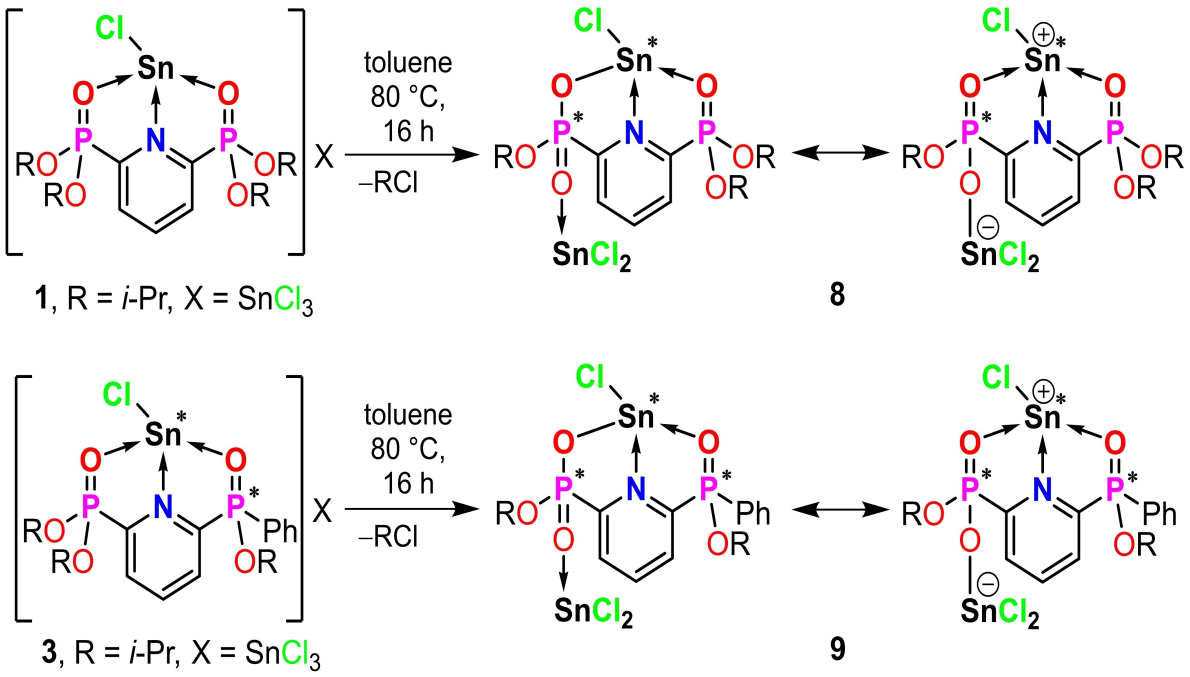

Scheme 6. Syntheses of compounds **8** and **9** by heating the tin salts **1** and **3**, respectively.

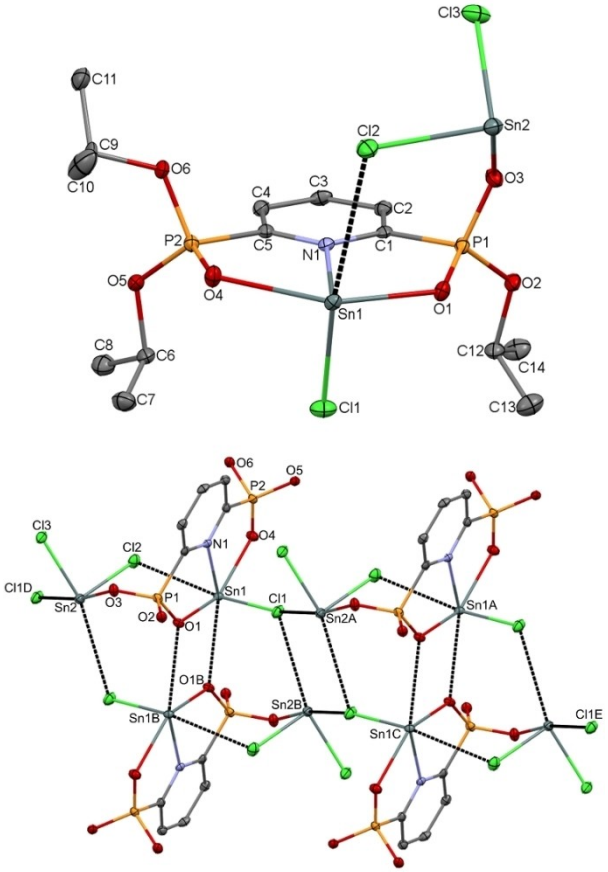

Figure 13. Molecular structure (upper part) and intermolecular connectivity (lower part) of compound **8** (ORTEP presentations at 50% probability of the depicted atoms and atom numbering scheme). The hydrogen atoms have been omitted for clarity. Selected interatomic distances (Å): Sn1-Cl1 2.5315(6), Sn1-Cl2 3.1297(6), Sn1-O1 2.2647(14), Sn1-O4 2.4437(14), Sn1-N1 2.4205(17), Sn1-O1B 3.1366(18), Sn2-Cl2 2.4633(6), Sn2-Cl3 2.4980(6), Sn2-O3 2.2691(15), P1-O1 1.5078(15), P1-O2 1.5745(15), P1-O3 1.5071(16), P2-O4 1.4808(16), P2-O5 1.5632(15), P2-O6 1.5596(15), Cl1-Sn2 A 3.1716(5), Cl1-Sn2B 3.631(5). Selected interatomic angles (°): Cl1-Sn1-Cl2 155.30(2), N1-Sn1-O1B 146.07(5), C1-P1-O1 105.30(9), P1-O1-Sn1 123.25(8), O1-Sn1-O4 145.91(5), Sn1-O4-P2 121.32(8), O4-P2-C5 108.45(9), P2-C5-N1 115.14(15), C5-N1-C1 118.21(18), C3-N1-Sn1 171.2(1), N1-C1-P1 114.66(15), P1-O3-Sn2 125.93(9), Sn1-Cl2-Sn2 111.65(2). Symmetry codes: [A] −1+x, y, z; [B] 1−x, 1−y, 2−z; [C] −x, 1−y, 2−z; [D] 1+x, y, z; [E] −1−x, 1−y, 2−z.

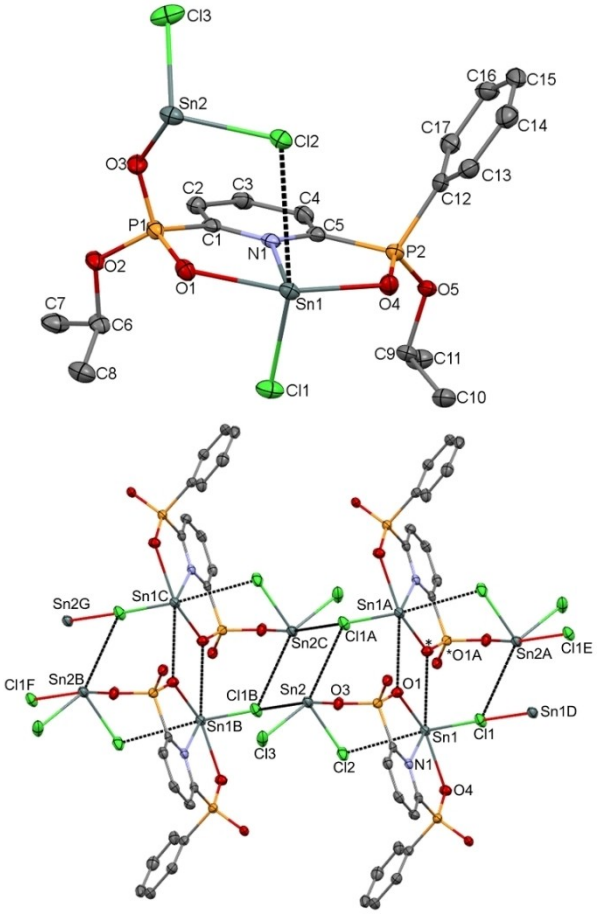

Figure 14. Molecular structure (upper part) and intermolecular connectivity (lower part) of compound **9** (ORTEP presentations at 50% probability of the depicted atoms and atom numbering scheme). The hydrogen atoms have been omitted for clarity. Selected interatomic distances (Å): Sn1-Cl1 2.5023(8), Sn1-Cl2 3.2649(9), Sn1-O1 2.265(2), Sn1-O4 2.430(2), Sn1-N1 2.425(2), Sn1-O1 A 3.2325(27), P1-O1 1.502(2), P1-O2 1.571(2), P1-O3 1.504(2), P2-O4 1.485(2), P2-O5 1.564(2), Sn2-O3 2.239(2), Sn2-Cl2 2.4968(8), Sn2-Cl3 2.4621(8), Sn2-Cl1 A 3.6889(11), Sn2-Cl1B 3.2597(7). Selected interatomic angles (°): Cl1-Sn1-Cl2 151.77(2), Sn1-O1-Sn1 A 112.76(9), O1-Sn1-O1 A 67.24(7), O3-Sn2-Cl1B 170.92(5), C1-P1-O1 105.52(13), P1-O1-Sn1 123.73(12), O1-Sn1-O4 146.00(7), Sn1-O4-P2 121.95(11), O4-P2-C5 107.54(13), P2-C5-N1 115.0(2), C5-N1-C1 118.4(3), C3-N1-Sn1 171.2(1), N1-C1-P1 115.0(2). Symmetry codes: [A] 1−x, 1−y, −z; [B] −1+x, y, z; [C] −x, 1−y, −z; [D] 1+x, y, z; [E] 2−x, 1−y, −z; [F] −2+x, y, z; [G] −1−x, 1−y, −z.

The thermal behaviour of compound **4** appeared more complex. Heating at reflux a suspension of **4** in toluene caused the greenish colour of the solid to change to colourless. Filtration and extraction with acetonitrile of the solid obtained gave the mono-heterocycle **10** as green crystalline material. After re-crystallization from DMSO respectively DMSO/THF of the solid precipitate from which **10** had been separated, the DMSO-coordinated bicyclic heterocycles **11** and **12** as greenish respectively colourless crystalline materials have been obtained (Scheme 7). Compound **10** shows moderate solubility in acetonitrile, and **11** and **12** are soluble in DMSO.

Figures 15–17 show the molecular structures of **10**-**12** and the corresponding figure captions contain selected interatomic distances and angles.

Compound **10** crystallized in the triclinic space group $P\bar{1}$ with one asymmetric unit in the unit cell. It is an intramolecularly N1→Sn1 (2.420(5) Å)- and O4→Sn1 (2.736(5) Å)-coordinated 2-carbmethoxy-6-carboxychlorostannyl(II)pyridine. It forms a centrosymmetric dimer via Sn1-O1 A interaction at an interatomic distance of 2.516(5) Å. The chlorine atoms in this dimer are trans. The dimers form an infinite two-dimensional coordination polymer by intermolecular Sn1-O2B/Sn1C–O2A and secondary Sn1-Sn1 C interactions at interatomic distances of 3.4684(51) and 4.0947(9) Å, respectively. The latter distance is even shorter than the corresponding distance in **7**.

From DMSO, compound **11** crystallized in the orthorhombic modification **11 a** (space group *P*bcn with four molecules in the unit cell). From DMSO/THF solution, crystals of the triclinic modification **11 b** (space group $P\bar{1}$ with two molecules in the unit cell) were obtained.

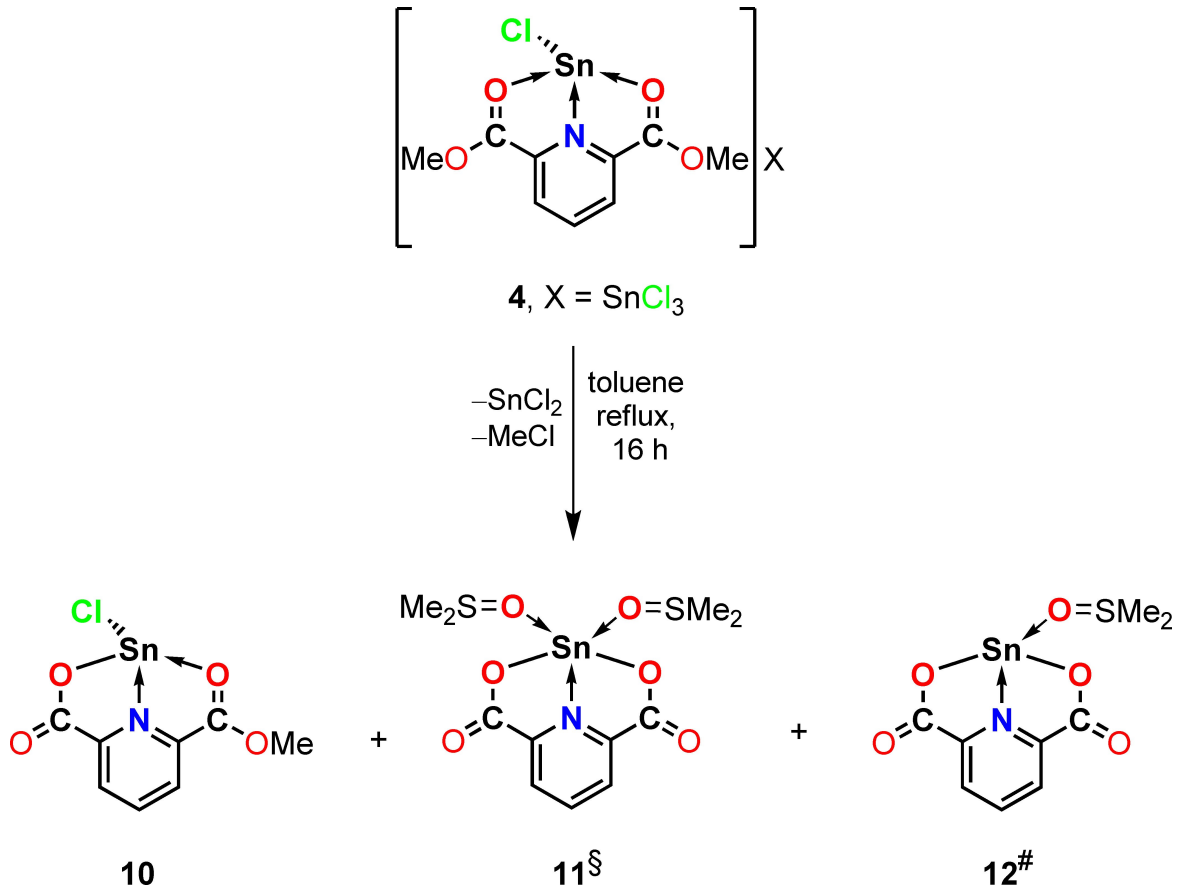

Scheme 7. Syntheses of compounds **11** and **12** by heating the tin salt **4**. [§]Obtained as orthorhombic (**11 a**) and triclinic (**11 b**) modifications by re-crystallization from DMSO respectively DMSO/THF of the precipitate formed in course of the reaction and from which compound **10** had been separated. [#]Also obtained by re-crystallization from DMSO/THF of the precipitate formed in course of the reaction and from which compound **10** had been separated.

In **11 a**, the Sn1 is five-coordinated in a strongly distorted a pseudo-octahedral coordination environment with O1, O1 A, N1 and the lone electron pair in the equatorial plane and the DMSO-oxygen atoms O2 and O2 A coordinating the Sn1 axially trans at a Sn1-O2 distance of 2.3802(12) Å. This distance is almost equal to the corresponding Sn–O distances of 2.382 (5) and 2.371 (5) Å reported for $[(Me_2SO)_2SnCl_2]_2$.[14b] The O2-Sn1-O2 A angle of 154.07(5)° reflects the stereochemical influence of the lone electron pair at the $Sn^{(II)}$ centre.

The major difference in the structure of **11 b** as compared to **11 a** is the formation of a centrosymmetric dimer in the former by weak intermolecular O→Sn interactions at a Sn1-O2 A distance of 3.373(1) Å being shorter than the sum of the van der Waals radii (3.69 Å)[12a–c] of the atoms involved. This gives the Sn1 a [5 + 1]-coordination in a distorted pseudo-pentagonal bipyramidal environment. The intramolecular interatomic distances in **11 a** and **11 b** fall within narrow ranges with the exception that in **11 b** as result of the intermolecular O→Sn interactions the intracyclic Sn1-O1 [2.3452(11) Å] and Sn1-O2 distances [2.2786(11) Å] differ. Also different is the Sn1-O2-S1 angle of 130.80(6)° in **11 a** versus the Sn1-O3-S1 [127.00(7)°] and Sn1-O4-S2 [113.76(6)°] angles in **11 b**.

The mono-DMSO-coordinated compound **12** crystallized in the monoclinic space group $P2_1/c$ with four asymmetric units in the unit cell. Unlike the doubly-DMSO-coordinated complex **11** (both modifications), **12** is a zig-zag shaped coordination polymer realized by intermolecular carboxylate bridging at Sn1-O5B distance of 2.4238(11) Å. The Sn1-O1 distance of 2.4248(11)Å is almost equal and indicates the carboxylate bridge being symmetric. This is further manifested by the almost equal C7-O1 and C7-O5 interatomic distances of 1.2589(17) and 1.2610(17) Å, respectively. The corresponding distances (Sn1-O2, C6-O2, C6-O4) for the carboxylate moiety being not involved in the bridging mode are quite different [2.2419(11), 1.2952(17), 1.2252(18) Å]. The Sn1-N1 and Sn1-O3 distances of 2.2775(12) and 2.3542(11) Å, respectively, are close or slightly shorter as compared to the corresponding distances in **11 a** and **11 b**. Like in **11 a**, the Sn1 in **12** shows a strongly distorted pseudo-octahedral coordination environment with the lone electron pair at Sn1 causing the O3-Sn1-O5B angle of 150.27(4) ° deviating from 180°.

In contrast to the P-containing compounds **8** and **9** which complex the $SnCl_2$ formed in course of the ester cleavage by intermolecular P=O→Sn coordination, no complexation of $SnCl_2$ by the C=O carboxylate oxygen atoms of compounds **10–12** is observed. A ^{119}Sn NMR spectrum of a solution in DMSO/THF (approx. 1:1) of the solid precipitate from which compound **10** had been removed by extraction with acetonitrile (vide supra)

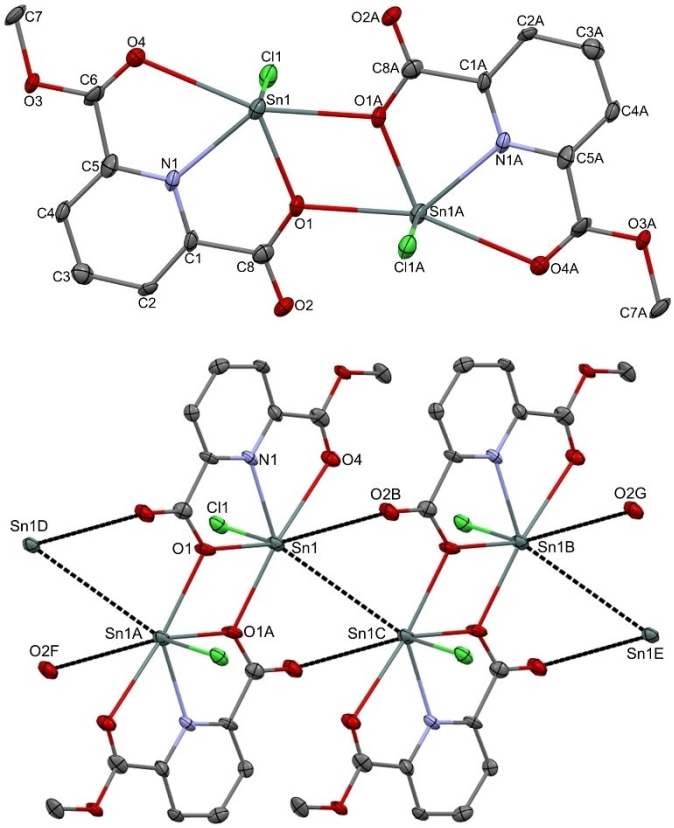

Figure 15. Molecular structure (upper part) and intermolecular connectivity (lower part) of compound **10** (ORTEP presentations at 50% probability of the depicted atoms and atom numbering scheme). The hydrogen atoms have been omitted for clarity. Selected interatomic distances (Å): Sn1-Cl1 2.4447(18), Sn1-O1 2.231(5), Sn1-O4 2.736(5), Sn1-N1 2.420(5), Sn1-O1 A 2.516(5), Sn1-O2B 3.4684(51), Sn1-Sn1 C 4.0947(9), C6-O3 1.314(8), C6-O4 1.200(8), C8-O1 1.286(8), C8-O2 1.208(8). Selected interatomic angles (°): C1-C8-O1 114.6(6), C8-O1-Sn1 119.1(4), O1-Sn1-O4 131.62(16), Sn1-O4-C6 114,87(46), O4-C6-C5 121.9(6), C6-C5-N1 114.2(6), C5-N1-C1 118.8(6), C3-N1-Sn1 172.7(1), C8-C1-N1 115.6(6), O1-Sn1-O2B 112.74(2), O4-Sn1-O1 A 160.04(2), Cl1-Sn1-Sn1 C 133.37(5). Symmetry codes: [A] 1−x, 1−y, 1−z; [B] −1+x, y, z; [C] −x, 1−y, 1−z; [D] 1+x, y, z; [E] −1−x, 1−y, 1−z; [F] 2−x, 1−y, 1−z; [G] −2+x, y, z.

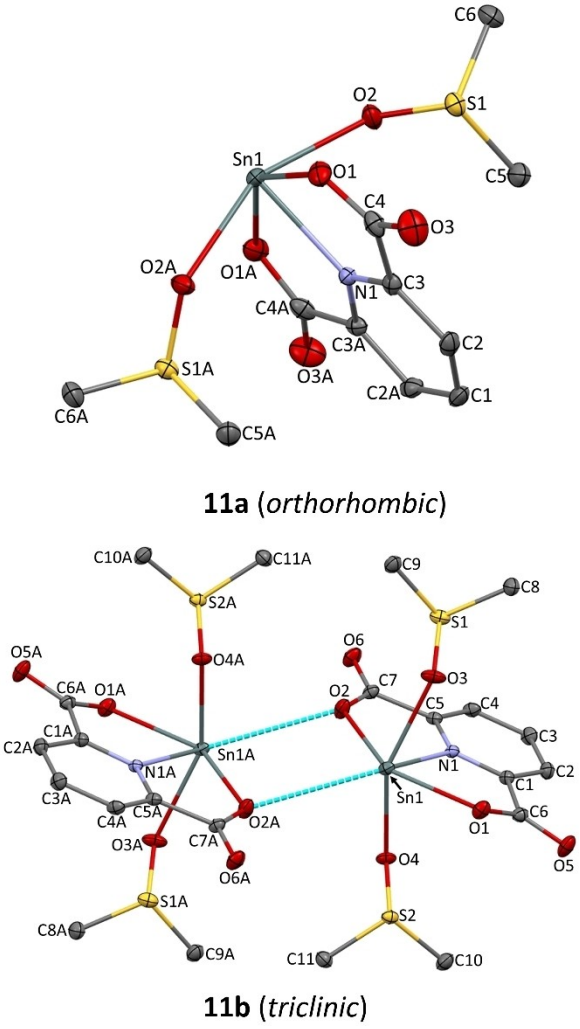

Figure 16. Molecular structures of the orthorhombic (**11 a**) and triclinic (**11 b**) modifications of compound **11** (ORTEP presentations at 50% probability of the depicted atoms and atom numbering scheme). The hydrogen atoms have been omitted for clarity. Selected interatomic distances (Å): **11 a**: Sn1-O1 2.2963(12), Sn1-O2 2.3802(12), Sn1-N1 2.2661(16), C4-O1 1.2783(17), C4-O3 1.2311(16), S1-O2 1.5305(11); **11 b**: Sn1-O1 2.3452(11), Sn1-O2 2.2786(11), Sn1-O2A 3.373(1), Sn1-O3 2.4046(12), Sn1-O4 2.3967(11), Sn1-O2A 3.373(1), Sn1-N1 2.2714(12), C6-O1 1.2793(19), C6-O5 1.2385(18), C7-O2 1.2849(18), C7-O6 1.2349(18), S1-O3 1.5368(11), S2-O4 1.5380(11) Selected interatomic angles (°): **11 a**: O1-Sn1-O1 A 139.88(5), O2-Sn1-O2 A 154.07(5), O1-C4-O3 126.59(13), O1-C4-C3 114.70(11), O3-C4-C3 118.72(13), Sn1-O2-S1 130.80(6), Sn1-O1-C4 120.99(8); **11 b**: O1-Sn1-O2 139.64(4), O3-Sn1-O4 151.58(4), N1-Sn1-O2A 115.06(4), O2-Sn1-O2 A 63.91(4), Sn1-O2-Sn1 A 116.09(4), O1-C6-O5 126.81(14), O1-C6-C1 115.04(13), O5-C6-C1 118.15(14), O2-C7-O6 126.39(14), O2-C7-C5 114.40(12), O6-C7-C5 119.21(13), Sn1-O3-S1 127.00(7), Sn1-O4-S2 113.76(6), N1-Sn1-O2 A 115.06(6). Symmetry codes: [A] 1−x, y, 1.5−z (for **11 a**); 1−x, 1−y, 2−z (for **11 b**).

showed a major intense broad signal at δ −336 ppm (integral 1.00, $\nu_{1/2}$ 3300 Hz), accompanied by low intense resonances at δ −420 and −427 (total integral of both signals 0.03), −624 (integral 0.011), and −659 ppm (integral 0.03). A ^{119}Sn NMR spectrum of $SnCl_2$ in the same solvent mixture revealed one single resonance at δ −332 ppm. With caution, the almost identical resonances (δ −336 and −332 ppm) indicate the formation of $SnCl_2$ in course of the ester cleavages according to Scheme 7.

Comparison of 11 a, 11 b, and 12 with Related Diorganotin(IV) Derivatives

There are several diorganotin(IV) derivatives of pyridine-2,6-dicarboxylic acid such as $[R_2Sn\{2,6\text{-}C_5H_3N(COO)_2\}(H_2O)]_2$ (R=Ph,[14c] *n*-Bu,[14d–g] vinyl,[14h]), $[Me_2Sn\{2,6\text{-}C_5H_3N(COO)_2\}(MeOH)]_2$[14i] and $[Me_2Sn\{2,6\text{-}C_5H_3N(COO)_2\}]_3$[14i] reported in the literature, in part as their aqua[14d] respectively chloroform[14g] solvates. The water- respectively methanol-coordinated derivatives dimerize via intermolecular O→Sn interactions involving the Sn*O*C(O) rather than the SnOC(*O*) oxygen atoms, similar as observed for **11 b**. The dimethyltin derivative[14i] lacking water or methanol coordination trimerizes via C=O→Sn bridges similar as observed for polymeric **12**, with the carboxylate moiety coordinating at Sn1-O11, Sn1-O12, and Sn3-O11 interatomic distances of 2.661(4), 2.415(4) and 2.462(4)

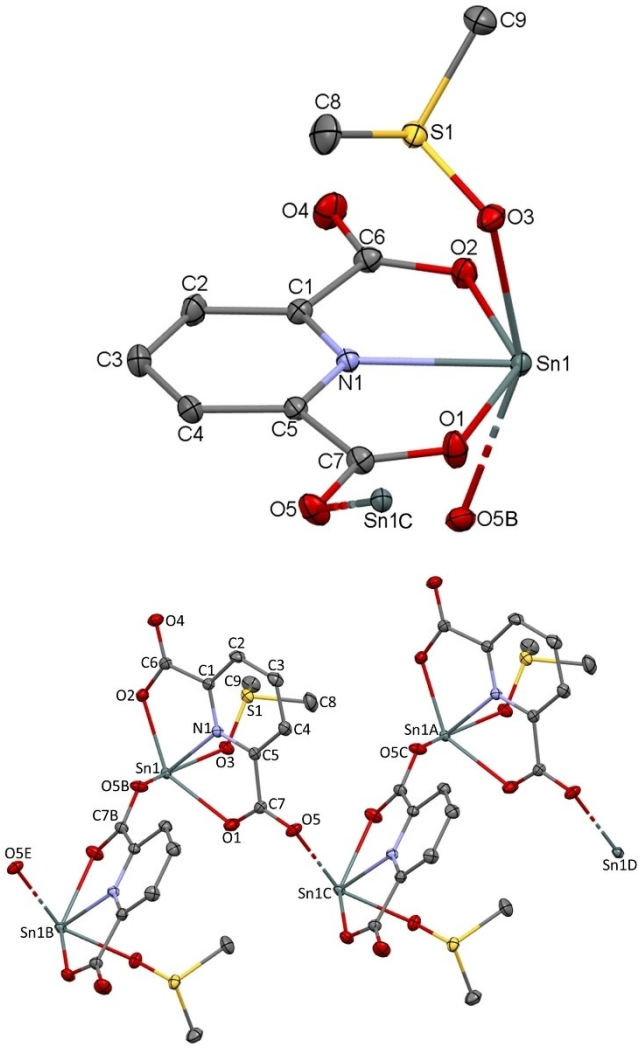

Figure 17. Structure in the solid state of compound **12** (ORTEP presentations at 50% probability of the depicted atoms and atom numbering scheme). The hydrogen atoms have been omitted for clarity. Selected interatomic distances (Å): Sn1-O1 2.4248(11), Sn1-O2 2.2419(11), Sn1-O3 2.3542(11), Sn1-O5B 2.4238(11), Sn1-N1 2.2775(12), C6-O2 1.2952(17), C6-O4 1.2252(18), C7-O1 1.2589(17), C7-O5 1.2610(17), S1-O3 1.5379(11). Selected interatomic angles (°): O1-Sn1-O2 139.45(4), O3-Sn1-O5B 150.27(4), Sn1-O5B–C7B 117.34(9), Sn1-O3-S1 124.57(6), Sn1-O1-C7 118.13(9), Sn1-O2-C6 121.56(9), O1-C7-O5 126.23(13), O1-C7-C5 116.78(12), C5-C7-O5 116.99(12), O2-C6-O4 126.34(14), O2-C6-C1 114.19(12), C1-C6-O4 119.47(13). Symmetry codes: [A] x, y, −1+z; [B] x, ½−y, ½+z; [C] x, ½−y, −½+z; [D] x, ½−y, 1½+z; [E] x, y, 1+z.

Å, respectively. The O11-C21 and O12-C21 interatomic distances are 1.255(6) and 1.242(7) Å. For more details including the distances for Sn2 and Sn3 see Supporting Information, Figure S77.

Reaction of the Stannylium Trichlorido Stannate 1 with $W(CO)_5$(thf)

The reaction (Scheme 8) of **1** with freshly prepared tungsten pentacarbonyl-thf complex $W(CO)_5$(thf), gave a yellow reaction mixture a ^{31}P NMR spectrum of which showed a single resonance at δ 13.4 ppm.

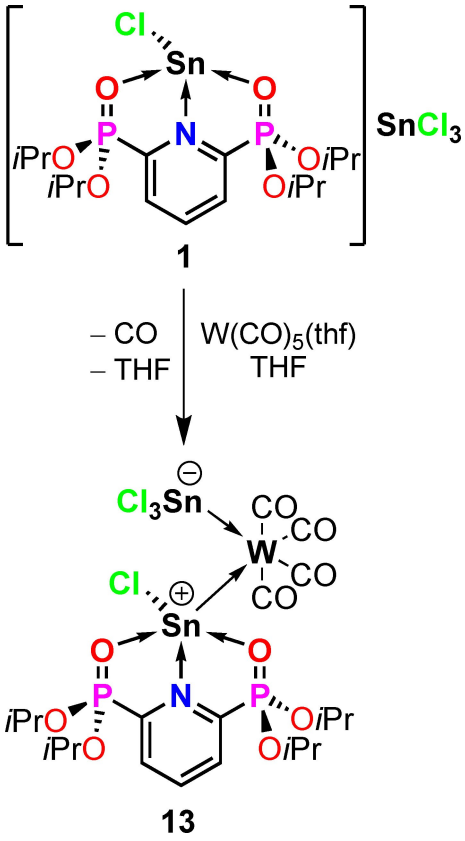

Scheme 8. Reaction of **1** with $W(CO)_5$(thf).

After the work-up procedure, a few single crystals of complex **13** suitable for X-ray diffraction analysis were obtained. Figure 18 shows its molecular structure and the figure caption contains selected interatomic distances and angles.

Complex **13** crystalized in the triclinic space group $P\bar{1}$ with two molecules per unit cell. The W(1) centre adopts a distorted octahedral environment, coordinated by four carbon monoxide ligands (C41-C44), the $SnCl_3^-$ anion and the L^1SnCl^+ cation with the two latter being *cis*. To the best of our knowledge, this is the first such example in which a tin(II) stannate anion and a tin(II) stannylium cation simultaneously coordinate to a transition metal centre. The Sn(1)–W(1) and Sn(2)–W(1) distances of 2.7070(4) and 2.6907(4) Å, respectively, are slightly shorter as reported for $(OC)_5WSn(OCH_2CH_2)_2NR$ [R=Me: 2.7275(12); R=*t*-Bu: 2.7490(5) Å][15] and also shorter than the sum of the covalent radii of tin and tungsten (2.77 Å).[12c] The Sn(1)–O(1), Sn(1)–O-(4), Sn(1)–N(1), and Sn(1)–Cl(1) distances of 2.233(3), 2.291(3), 2.336(3), and 2.3656(12) Å, respectively, are shorter as compared to the corresponding distances in the parent compound **1**. Apparently, coordination to the tungsten centre increases the Lewis acidity of the stannylium L^1SnCl^+ cation.

DFT Calculations

To gain a deeper understanding of the electronic structure of the complexes **1**, **3**, **6**, **8**, **9**, **10** and **13** density functional theory

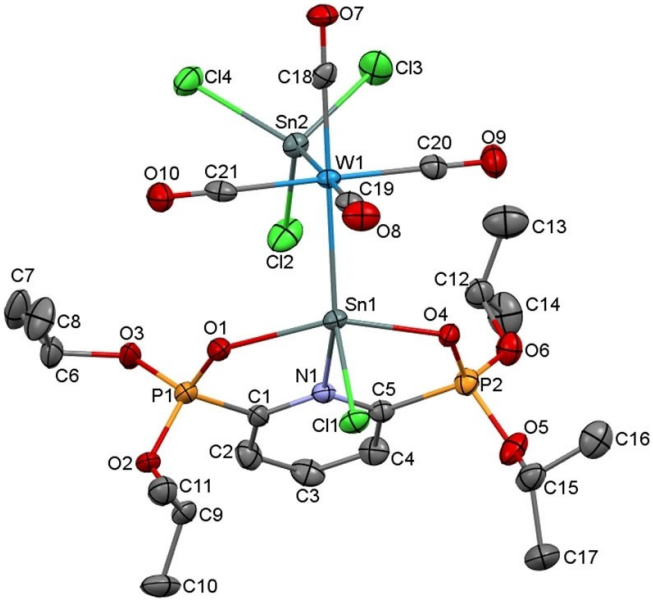

Figure 18. Molecular structure (upper part) and intermolecular connectivity (lower part) of compound **13** (ORTEP presentations at 50% probability of the depicted atoms and atom numbering scheme). Hydrogen atoms have been omitted for clarity. Selected interatomic distances (Å): Sn1-W1 2.7070(4), Sn1-Cl1 2.3656(12), Sn1-O1 2.233(3), Sn1-O4 2.291(3), Sn1-N1 2.336(3), P1-O1 1.485(3), P1-O2 1.545(3), P1-O3 1.541(4), P2-O4 1.486(3), P2-O5 1.551(4), P2-O6 1.541(3), Sn2-W1 2.6907(4), W1- C18 1.972(5), W1-C19 1.980(5), W1-C20 2.013(5), W1-C21 2.044(5). Selected interatomic angles (°): Sn1-W1-Sn2 91.085(11), Cl1-Sn1-W1 130.96(3), N1-Sn1-W1 138.33(9), C1-P1-O1 105.6(2), P1-O1-Sn1 124.44(18), O1-Sn1-O4 148.28(11), Sn1-O4-P2 123.84(18), O4-P2-C5 105.3(2), P2-C5-N1 115.4(3), C5-N1-C1 118.4(4), C3-N1-Sn1 176.7(1).

(DFT) calculations and natural bond orbital (NBO) analyses,[16] and furthermore for compound **13** an energy decomposition analysis (EDA)[17] were performed. The calculated structures with the functional TPSSh[18] with the basis set def2-TZVP [19] and with an effective core potential (ECP) for the heavier atoms Sn[20a] and W[20b] and empirical dispersion correction with Becke-Johnson damping[21] are in agreement with the molecular structures determined for the solid state by single X-ray diffraction analysis (see Tables S4–S7). Table S8 contains the NBO charges for selected atoms of the complexes **1**, **3**, **6**, **8**, **9**, **10**, and **13**. Except for **13**, the NBO charges for the tin centres in the $[L^nSnCl]^+$ cations are in the range of 1.24 to 1.29 e units and 0.98 to 1.19 e units for the Sn centres of the $SnCl_3^-$ anions. In accordance with a previous study[22a] the NBO charges of 1.24 to 1.29 e units indicate the Sn in $[L^nSnCl]^+$ to be in the oxidation state +II. The Sn–Cl bonds in the $SnCl_3^-$ anions exhibit more covalent character. Consequently, the NBO charges of 0.98 to 1.19 e units define the oxidation state of the Sn centres in these to be +II as well.

The charge transfer energies obtained by NBO analysis (Table S8) together with the Wiberg bond order indices (Table S9) give an impression about the covalency of the corresponding bonds. The Sn–Cl bonds have a more covalent character whereas the N→Sn or O→Sn interactions are donor acceptor interactions. The N→Sn or O→Sn interactions are in the same range of electron density donation to the Sn atom (e.g. 46 kcal/mol for the N→Sn interaction and 44–47 kcal/mol for the O→Sn interactions in compound **1**).

In complex **13**, the NBO charge (Table S8) of the Sn in the $[L^1SnCl]^+$ cation is +1.55 e units and therefore higher than the NBO charges of the tin centres in the $[L^nSnCl]^+$ cations in the complexes discussed above. It imposes the question after the oxidation state for this Sn^+ cation. In addition, the NBO analysis revealed a 3-center-4-electron bond between the Sn and the W atom and the CO groups. Thus, the bond order calculation is difficult. Figure 19 depicts the three possible oxidation states for the W and Sn centres in compound **13**: (i) both cationic and anionic moieties with Sn(II) and W(0), (ii) cationic moiety with Sn(III), anionic moiety with Sn(II) and W(−I), and (iii) cationic moiety with Sn(IV), anionic moiety with Sn(II) and W(−II).

With the energy decomposition analysis of the fragment-based wavefunction methodology the orbital interaction energy E_{orb} can be determined. The fragmentation with the smallest E_{orb} represents the best chemical description of the complex. For the complex **13**, this is the case for the situation with Sn(II) for both the cationic and anionic moieties, and W(0) for the tungsten tetracarbonyl moiety.

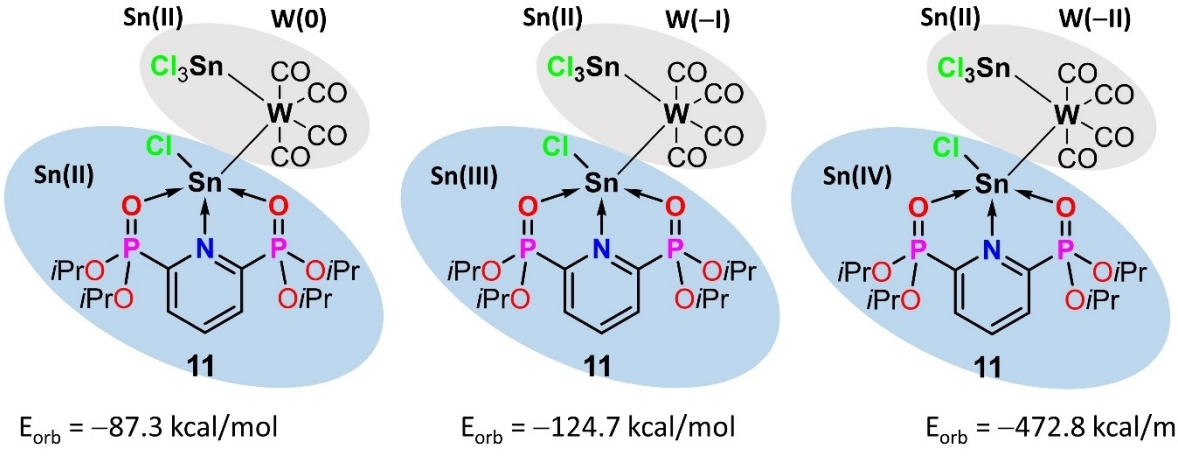

E_{orb} = −87.3 kcal/mol E_{orb} = −124.7 kcal/mol E_{orb} = −472.8 kcal/mol

Figure 19. Fragmentation schemes of compound **13** for EDA analyses and the values for the orbital interaction energy for each possible fragmentation.

The natural bond orbitals are more localized than the canonical orbitals. Thus, the lone pairs of the Sn atoms of the cations are depicted in Figure 20. In all complexes, the Sn lone pairs possess more than 90% of s-character and only small amounts of p-character (Table S10).

In complex **13**, there is the lone pair of the Sn^+ cation with similar contributions (92.7% s-character and 7.2% p-character) as in the other complexes **1**, **3**, **6**, **8**, **9** and **10** (Figure 21, Table S10). Two d orbitals of the W atoms are responsible for the electron density interaction to the Sn^+ cation and the $SnCl_3^-$ anion.

Conclusions

Tridentate pyridine-backboned O,N,O-coordinating chelating ligands L^n with phosphonate (n = 1), phosphinate (n = 2), carboxylate (n = 3) and carbamide substituents (n = 4), respectively, react with tin(II) halides, SnX_2 (X=Cl, Br), under autoionization giving salts of the type $[L^nSnX]SnX_3$. In these, the intramolecular Sn–N distances vary between 2.316(2) (for **6**, n = 4) and 2.526(4) (for **1**, n = 1; Table S11) reflecting the corresponding $[L^nSnX]^+$ cations to have different strength of Lewis acidity which is relevant for the activity of these compounds as catalysts for polyurethane formation.[22b] The Sn–X and Sn–O distances (Table S11) vary as well as does vary the interionic connectivity in the crystal structures of these salts. A remarkable feature of the crystal structures are secondary Sn···Sn interactions for **6** and **10** at distances smaller than twice the van der Waals radius of this atom. Upon heating of the salts **1** and **3** partial cleavage of P–O bonds take place giving the intramolecularly P=O→SnCl- and N→SnCl-coordinated as well as intermolecularly P=O→$SnCl_2$-coordinated five-membered heterocycles **8** and **9**, respectively. In course of these reactions

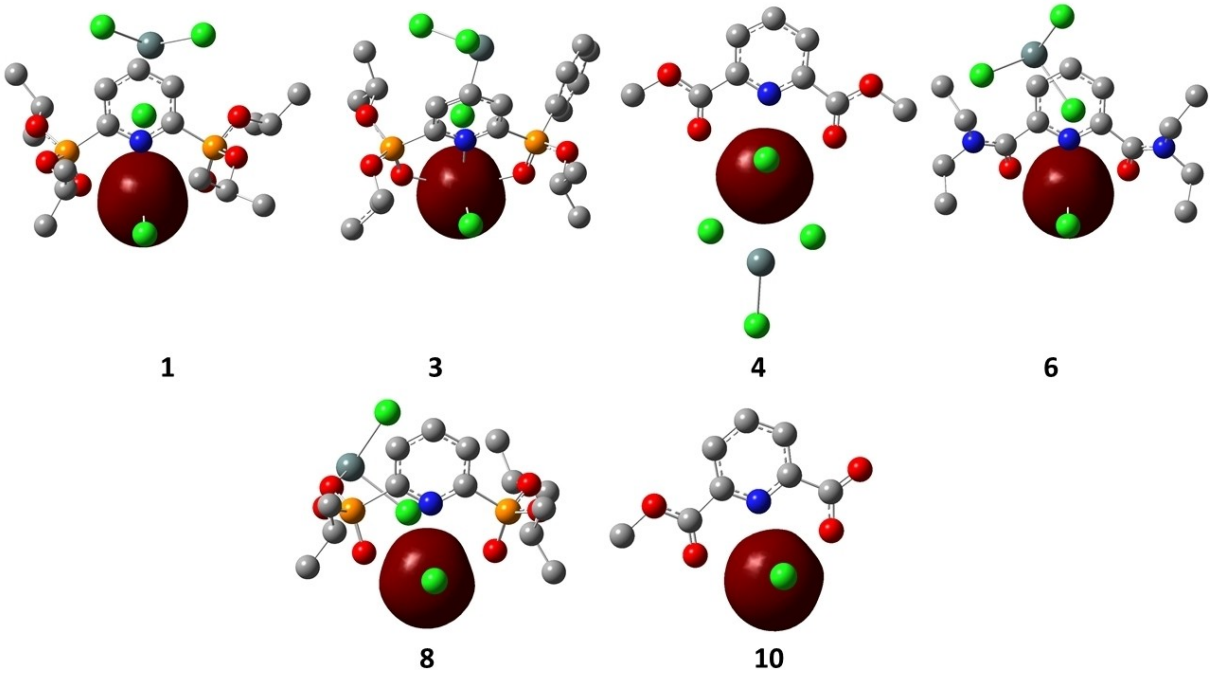

Figure 20. NBO of the lone electron pair at Sn in the complexes **1**, **3**, **6**, **8**, **9** and **10** (NBO6.0, TPSSh/def2-TZVP/ECP/GD3BJ, isovalue 0.04).

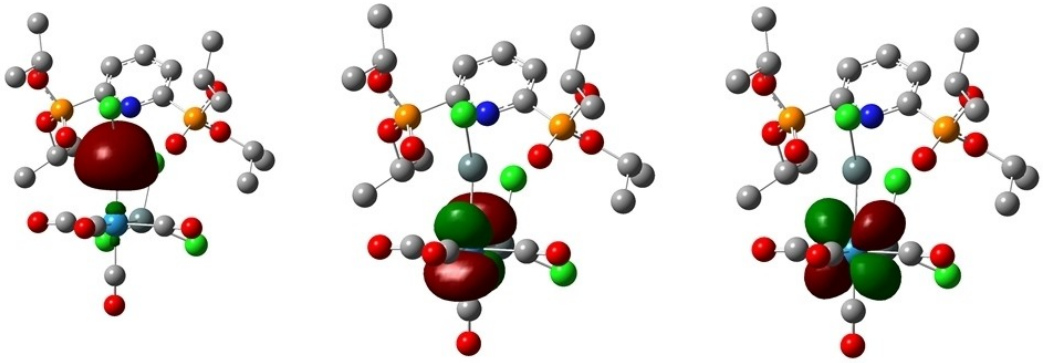

Figure 21. NBO of the lone electron pair at Sn (left) and the orbitals responsible for the electron density interaction of the W atom (middle and right) in complex **13** (NBO6.0, TPSSh/def2-TZVP/ECP/GD3BJ, isovalue 0.04).

stereogenic centres at the P atoms are formed. Heating of the salt **4** caused cleavage of one as well as both ester functions giving the five-membered heterocycle **10** and the DMSO-coordinated bicyclic tin(II) derivatives **11** and **12**. Unprecedentedly, the salt $[L^1SnCl]SnCl_3$ (**1**) proved to act as a "double ligand" in its reaction with tungsten tetracarbonyl giving a complex containing both the $SnCl_3^-$ anion and the $[L^1SnCl]^+$ cation. DFT calculation reveals both tin centres in this complex being Sn(II).

The results presented in this manuscript encourage future works concerning (i) studying the stereoselectivity of the ester cleavage under formation of stereogenic centres, (ii) the elucidation of the mechanism operative for this ester cleavage, (iii) the hydrolysis of the heterocycles **8**–**10** to give the corresponding acids (for **8** and **9** stereoselective), and (iv) to evaluate in more detail the complexation behaviour of the salts towards transition metal compounds.

Experimental

General

All reactions were carried out under an argon atmosphere using standard Schlenk line technique, unless otherwise specified. The argon was dried by passing through a glass column filled with phosphorus pentoxide and the glassware was dried by flame under reduced pressure. All solvents were dried according to standard procedures, freshly distilled and stored over molecular sieve.[23] The dimethyl pyridine-2,6-dicarboxylate (ligand **L3**) was purchased from BLD Pharmatech GmbH. The bis(diethylamino) pyridine-2,6-dicarboxylate (ligand **L4**) was synthesized as reported in the literature.[24]

The NMR spectra were measured at room temperature (unless as otherwise stated) using the spectrometers Bruker AV 400 Avance III HD NanoBay, AV 500 Avance NEO, AV 600 Avance III HD, Agilent Technologies DD2. The NMR chemical shifts (δ) are given in ppm and the coupling constants J in Hz. ^{1}H and ^{13}C{^{1}H} NMR chemical shifts were referenced against $SiMe_4$ via the chemical shift of the solvents (C_6D_6 ^{1}H 7.16, ^{13}C 128.39, CD_2Cl_2 ^{1}H 5.32, ^{13}C 54.00, $CDCl_3$ ^{1}H 7.26, ^{13}C 77.16, CD_3CN ^{1}H 1.94, ^{13}C 1.39, CD_3OD ^{1}H 3.31, ^{13}C 49.00).[25] The ^{31}P and ^{119}Sn NMR spectra were referenced against 85 % H_3PO_4 and $SnMe_4$, respectively. The IR spectra (cm^{-1}) were measured as a solid or oil on ATR Perkin Elmer and Bruker Alpha II Platinum-ATR spectrometers. The melting point (°C) was determined by a Büchi M-560 device using an opened capillary. The elemental analyses were performed under non-inert conditions on a Leco CHNS-932 analyzer. The electrospray mass spectra were recorded using a Thermoquest Finnigan Instrument. The mobile phase was acetonitrile or dichloromethane with a flow rate of 10 μL/min; concentration $c = 0.1\ mg \cdot mL^{-1}$, source voltage 3.8 kV, capillary voltage 41 V (tube lens: 140 V), capillary temperature 275 °C.

Crystallography

Intensity data for the crystals of **1**–**10** and **13** were collected on Xcalibur2 CCD (Oxford Diffraction) with graphite-monochromated MoKα (0.71073 Å) radiation at 173(1) K.

The data of **11a**, **11b**, and **12** were collected on a Bruker D8 VENTURE diffractometer with an Incoatec Iμs 3.0 microfocussed Ag Kα source with mirror optics. The Hybrid Pixel Array Detector (HPAD) used was a Bruker PHOTON III. Data collection was performed with APEX5 (with integrated programs SAINT for integration and SADABS for absorption correction). SHELXT was used for the solution and refinement of the crystal structures. OLEX2 was used for processing and finalization of the crystal structures. The mounting of the crystals was performed with *MiTeGen MicroMounts*.

Crystal decay was monitored by repeating the initial frames at the end of data collection. The data were corrected using multi-scans. The structures were solved by direct methods SHELXS97[26] and successive difference Fourier syntheses. Refinement applied full-matrix least-squares methods SHELXL2018.[27] In compound **L2**^{i} the *i*-propyl substituent attached to O(3) is disordered over three positions with an occupancy 40:40:20. The *i*-propyl substituent attached to O(3) of compound **11** is also disordered over two positions with an occupancy of 55:45. The H atoms were placed in geometrically calculated positions using a riding model with U_{iso} constrained at 1.2 for non-methyl and 1.5 for methyl groups times U_{eq} of the carrier C atom. Atomic scattering factors for neutral atoms and real and imaginary dispersion terms were taken from *International Tables for X−ray Crystallography[1]*.[28] The figures were created using the program MERCURY. The Supporting Information (Tables S1-S3) contain the crystallographic data.

The CCDC deposition numbers 2286126 (**1**), 2286127 (**1**·C_7H_8), 2286128 (**2**), 2286129 (**3**) −2286130 (**4**) 2286131 (**5**·CH_3CN), 2286132 (**6**), 2286133 (**7**), 2286134 (**8**), 2286135 (**9**) 2286136 (**10**), 2348638 (**11a**), 2348639 (**11b**), 2350019 (**12**), 2286137 (**13**), 2326214 (**L2**^{i}), and 2326215 (**4**·CH_3CN) contain the supplementary crystallographic data for this paper. These data are provided free of charge by the joint Cambridge Crystallographic Data Centre and Fachinformationszentrum Karlsruhe at http://www.ccdc.cam.ac.uk/structures or by emailing data_request@ccdc.cam.ac.uk, or by contacting The Cambridge Crystallographic Data Centre, 12 Union Road, Cambridge CB2 1EZ, UK; fax: +441223336033.

Density Functional Theory (DFT)

DFT calculations were performed with Gaussian 16, Revision C01.[29] The geometry optimizations were started from the geometry of the solid-state structures using the TPSSh functional[18] and with the Ahlrichs type basis set def2-TZVP[19] basis set as implemented in Gaussian 16, Revision C01.[29] For the heavier atoms Sn and W effective core potentials (ECP) were used.[20] NBO calculations were accomplished using the program suite NBO 6.0 delivering the NBO charges and the charge-transfer energies by second order perturbation theory.[16] As empirical dispersion correction, we used the D3 dispersion with Becke-Johnson damping as implemented in Gaussian16, Revision B.01.[21] The energy decomposition analysis (EDA) of Morokuma and Ziegler[17] was performed with the program AOMix.[30]

Synthesis of 2,6-{P(O)(OiPr)$_2$}C_5H_4N, L1

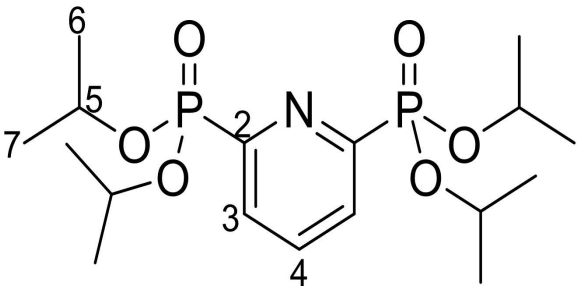

Numbering scheme for L1

The ligand **L1** was synthesized according to a slightly modified procedure reported by E. A. Konopkina, W.-Q. Shi et al.[11b] To a solution containing 2,6-dibromopyridine (20.00 g, 84.4 mmol), di*iso*-propyl phosphite (33.70 g, 202.6 mmol) and triethylamine (42.70 g, 422.0 mmol) in acetonitrile (500 mL) were added at room temperature palladium(II)acetate (0.19 g, 0.8 mmol) and dppf (0.51 g, 0.9 mmol). The reaction mixture was heated at 100 °C for 48 h. After the solid had been filtered and the solvent removed under reduced pressure, the residue was dissolved in ethyl acetate (50 mL). Water (100 mL) was added and the organic layer was separated. The aqueous layer was extracted with ethyl acetate (3x, 50 mL). Then, the combined organic layers were dried over $MgSO_4$, filtrated and concentrated to dryness. The crude product was purified by chromatography (ethyl acetate as eluent) to obtain a brown solid (yield 30.55 g, 88 %) of m.p. 53.8 °C. It decomposes at 228 °C. **^{1}H NMR** (400.25 MHz, CD_2Cl_2): δ 7.91-7.95 (complex pattern, 2H, H3), 7.78-7.84 (complex pattern, 1H, H4), 4.65-4.76 (superimposed doublet of septets,, 4H, OC*H*), 1.28 (d, $^3J(^1H–C–C–^1H) = 6$ Hz, 12H, CH_3), 1.19 (d, $^3J(^1H–C–C–^1H) = 6$ Hz, 12H, CH_3), (400.25 MHz, C_6D_6): $\delta = 7.89–7.93$ (complex pattern, 2H, H3), $\delta = 6.93–7.00$ (complex pattern, 1H, H4), 4.79–4.90 (superimposed doublet of septets,, 4H, OC*H*), 1.23 (d, $^3J(^1H–C–C–^1H) = 6$ Hz, 12H, CH_3), 1.16 (d, $^3J(^1H–C–C–^1H) = 6$ Hz, 12H, CH_3), **^{13}C{^{1}H} NMR** (100.64 MHz, CD_2Cl_2): δ 154.7 [dd, $^1J(^{13}C–^{31}P) = 224$ Hz, $^3J(^{13}C–N–C–^{31}P) = 21$ Hz, C2], 136.5 (t, $^3J(^{13}C–C–C–^{31}P) = 11$ Hz, C4), 129.7 [dd, $^2J(^{13}C–C-^{31}P) = 25$ Hz, $^4J(^{13}C–C–C–C–^{31}P) = 4$ Hz, C3), 72.2 (complex pattern, OC*H*, C5), 24.2 (complex pattern, CH_3, C6), 24.0 (complex pattern, CH_3, C7), (100.64 MHz, C_6D_6): $\delta = 154.8$ [dd, $^1J(^{13}C–^{31}P) = 224$ Hz, $^3J(^{13}C–N–C–^{31}P) = 21$ Hz, C2], 136.1 (t, $^3J(^{13}C–C–C–^{31}P) = 11$ Hz, C4), 129.0 [dd, $^2J(^{13}C–C–^{31}P) = 25$ Hz, $^4J(^{13}C–C–C–C–^{31}P) = 4$ Hz, C3), 71.2 (complex pattern, OC*H*, C5), 23.8 (complex pattern, CH_3, C6), 23.6 (complex pattern, CH_3, C7),**^{31}P{^{1}H} NMR** (162 MHz, C_6D_6): δ 7.7 [s, $^1J(^{31}P-^{13}C) = 223$ Hz], CD_2Cl_2: δ 7.3 [$^1J(^{31}P-^{13}C) = 224$ Hz]; **IR spectroscopy**: $\tilde{\nu}_{(P=O)}$ 1247 cm^{-1}; **Elemental Analyses**. Calcd. for $C_{17}H_{31}NO_6P_2$ (407.38 g/mol): C 50.12, H 7.67, N 3.44 %. Found: C 49.9, H, 7.6, N, 3.2 %. **ESI-MS** (70 eV, positive mode): m/z (%): 408.2 (90) [M + H$^+$].

Synthesis of 2-Br-6-{P(O)(OiPr)$_2$}C$_5$H$_4$N, L2^i

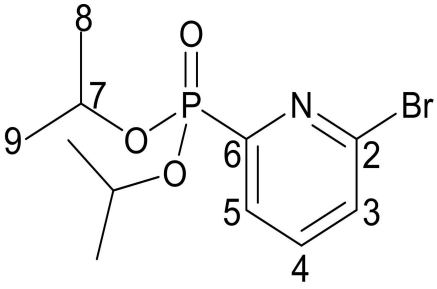

Numbering scheme for L2^i

To a solution containing 2,6-dibromopyridine (10.00 g, 42.1 mmol), di*iso*propyl phosphite (7.01 g, 42.1 mmol) and triethylamine (13.00 g, 126.6 mmol) in acetonitrile (250 mL) were added at room temperature palladium(II)acetate (0.1 g, 0.4 mmol) and dppf (0.25 g, 0.4 mmol). The reaction mixture was heated at 100 °C for 48 h. After the solid had been filtrated and the solvent removed under reduced pressure, the residue was dissolved in ethyl acetate (20 mL). Water (50 mL) was added and the organic layer was separated. The aqueous layer was extracted with ethyl acetate (3x, 20 mL). The combined organic layers were dried over $MgSO_4$, filtrated and the filtrate evaporated to dryness. The crude product was purified by column chromatography (ethyl acetate as eluent) to obtain a brown solid (yield 11.29 g, 83 %). **^{1}H NMR** (400.25 MHz, $CDCl_3$): δ 7.87 [superimposed dd, $^3J(^1H–C–C–^1H) = 7.3$ Hz, 6.4 Hz, 1H, H4), 7.54 – 7.64 (complex pattern, 2H, H3 and H5), 4.48 (superimposed doublet of septets, 2H, OC*H*, H7), 1.37 [d, $^3J(^1H–C–C–^1H) = 6$ Hz, 12H, CH_3, H8], 1.30 [d, $^3J(^1H–C–C–^1H) = 6$ Hz, 12H, CH_3, H8] **^{13}C{^{1}H} NMR** (100.6 MHz, $CDCl_3$): δ 154.6 [d, $^1J(^{13}C-^{31}P) = 227$ Hz, C6], 142.8 (d, $^3J(^{13}C–N–C–^{31}P) = 25$ Hz C2), 138.2 [d, $^2J(^{13}C, ^{31}P) = 12$ Hz, C5], 130.5 (s, C3), 126.7 [d, $^3J(^{13}C–N–C–^{31}P) = 24$ Hz C4], 72.3 [d, $^2J(^{13}C–O–^{31}P) = 6$ Hz, C7], 24.0 [d, $^3J(^{13}C–O–C–^{31}P) = 4$ Hz, C8], 23.7 (d, $^3J(^{13}C–O–C–^{31}P) = 5$ Hz, C9), **^{31}P{^{1}H} NMR** (162 MHz, $CDCl_3$): δ 6.5 (s). No elemental analysis was performed.

Synthesis of 2-{P(O)(OiPr)$_2$}-6-{P(O)(OiPr)Ph}C$_5$H$_4$N, L2

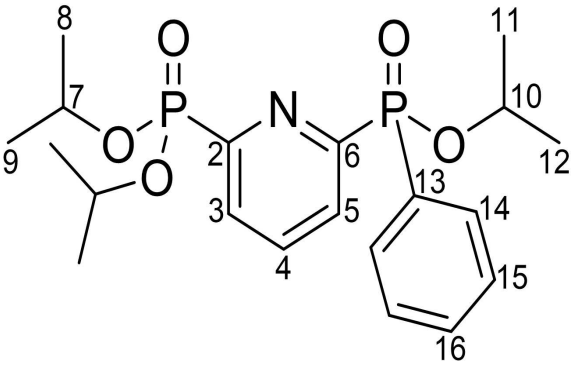

Numbering scheme for compound L2

To a solution of 2-(diisopropyl phosphonato)-6-bromo pyridine (10.00 g, 31.0 mmol), *iso*propyl phenyl phosphite (5.72 g, 31.0 mmol) and triethylamine (6.00 g, 31.0 mmol) in acetonitrile (250 mL) was added at room temperature palladium(II)acetate (0.1 g, 0.4 mmol) and dppf (0.25 g, 0.4 mmol). The reaction mixture was heated for 48 h at 100 °C. After the solid had been filtered and the solvent removed under reduced pressure, the residue was dissolved in ethyl acetate (20 mL). Water (50 mL) was added and the organic layer was separated. The aqueous layer was extracted with ethyl acetate (3x, 20 mL). The combined organic layers were dried over $MgSO_4$ followed by complete removal of the solvent. The crude product obtained was purified by column chromatography (ethyl acetate as eluent) to obtain a brown solid (yield 8.50 g, 85 %). **^{1}H NMR** (400.25 MHz, C_6D_6): δ 8.26 (complex pattern, 2H, H14), 8.18 (complex pattern, 1H, H3), 7.88 (complex pattern, 1H, H5), 7.08 (complex pattern 3H, H15 + H16), 7.04 (complex pattern, 1H, H4), 4.79 (superimposed doublet of septets, 1H, OC*H*), 4.68 (superimposed doublet of septets, 1H, OC*H*), 4.57 (superimposed doublet of septets 1H, OC*H*), 1.22 [d, $^3J(^1H–C–C–^1H) = 6$ Hz, 3H, CH_3], 1.20 [d, $^3J(^1H–C–C–^1H) = 6$ Hz, 3H, CH_3], 1.18 [d, $^3J(^1H–C–C–^1H) = 6$ Hz, 3H, CH_3], 1.13 [d, $^3J(^1H–C–C–^1H) = 6$ Hz, 3H, CH_3], 1.08 [d, $^3J(^1H–C–C–^1H) = 6$ Hz, 3H, CH_3], 0.99 [d, $^3J(^1H–C–C–^1H) = 6$ Hz, 3H, CH_3], **^{31}P{^{1}H} NMR** (162 MHz, C_6D_6): δ 7.2 (s), 22.3 (s). No elemental analysis was performed.

Synthesis of compounds 1–7

Compounds **1**–**7** were synthesized in 85–90 % yield by stirring $SnCl_2$ with the corresponding ligand (molar ratio 2 : 1) at room temperature in toluene (for **1**–**3**), acetonitrile (for **4** and **5**) and methanol (for **6** and **7**).

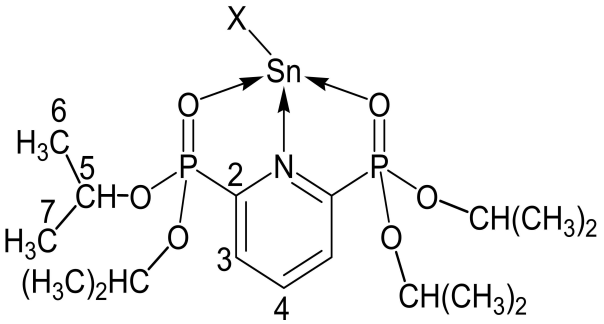

Numbering scheme for compounds 1 and 2. The $SnCl_3^-$ is omitted.

$$[\mathbf{2,6}\text{-}\{\mathbf{P(O)(O}i\mathbf{Pr})_2\}\mathbf{C_5H_3NSnCl}]\mathbf{SnCl_3} \quad (1)$$

Isolated as colourless crystals of m.p. 71 °C. **^{1}H NMR** (400 MHz, CD_2Cl_2): δ 8.63 (complex pattern, 1H, H4), 8.30 (complex pattern, 2H, H3), 5.07 (superimposed doublet of septets, 4H, OC*H*), 1.49 [d, ^3J(^{1}H–C–C–^{1}H) = 6 Hz, 12H, CCH_3], 1.31 [d, ^3J(^{1}H–C–C–^{1}H) = 6 Hz, 12H, CCH_3).

^{13}C{^{1}H} NMR (150.94 MHz, CD_2Cl_2): δ 147.8 [dd, ^1J(^{13}C-^{31}P) = 217 Hz, ^3J(^{13}C–N–C–^{31}P) = 18 Hz, C2], 143.0 [t, ^3J(^{13}C–C–C–^{31}P) = 9 Hz, C4], 132.8 [dd, ^2J(^{13}C–C–^{31}P) = 19 Hz, ^4J(^{13}C-^{31}P) = 3 Hz, C3], 77.2 [d, ^2J(^{13}C–O–^{31}P) = 6 Hz, OCH], 24.0 [d, ^3J(^{13}C–O–C–^{31}P) = 3 Hz, CCH_3], 23.9 [d, ^3J(^{13}C–O–C–^{31}P = 5 Hz, CCH_3]. **^{31}P{^{1}H} NMR** (162 MHz, CD_2Cl_2): δ 16.5 [s, ^1J(^{31}P-^{13}C) = 221 Hz]. **^{31}P{^{1}H} NMR** (162 MHz, CD_2Cl_2, T = 193 K): δ 17.9 [s, ^1J(^{31}P–^{13}C) = 210 Hz]. **^{119}Sn{^{1}H} NMR** (149 MHz, CD_2Cl_2, T = 193 K): δ −90 (s, *Sn*Cl_3^-), −701 (s, *Sn*Cl^+). **IR spectroscopy**: $\tilde{\nu}_{(P=O)}$ 1207 cm^{-1}. **Elemental analysis** calcd. for $C_{17}H_{31}Cl_4NO_6P_2Sn_2$ (786.61 g/mol): C 25.96, H 3.97, N 1.78%, found: C 25.9, H 4.0, N 1.8%; **ESI-MS** (70 eV, positive mode): m/z (%) 385.1 [$C_{14}H_{28}N_1O_7P_2$]; (negative mode): 482.7 [$C_5H_9N_1O_7P_2SnCl_3$].

$$[\mathbf{2,6}\text{-}\{\mathbf{P(O)(O}i\mathbf{Pr})_2\}\mathbf{C_5H_3NSnBr}]\mathbf{SnBr_3} \quad (2)$$

Isolated as pale yellow solid which decomposed at 123 °C. **^{1}H NMR** (400 MHz, CD_2Cl_2): δ 8.62 (complex pattern, 1H, H4), 8.29 (complex pattern, 2H, H3), 5.10 (complex pattern, 4H, OC*H*), 1.49 [d, ^3J (^{1}H–C–C–^{1}H) = 6.2 Hz, 12H, CCH_3], 1.32 [d, ^3J (^{1}H–C–C–^{1}H) = 6.2 Hz, 12H, CCH_3].

^{13}C{^{1}H} NMR (101 MHz, CD_2Cl_2): δ 148.2 [dd, ^1J(^{13}C-^{31}P) = 218 Hz, ^3J(^{13}C–N-C-^{31}P) = 18 Hz, C2], 142.9 [t, ^3J(^{13}C–C–C–^{31}P) = 10 Hz, C4], 132.9 [dd, ^2J(^{13}C–C-^{31}P) = 19 Hz, ^4J(^{13}C-^{31}P) = 3 Hz, C3], 77.5 (d, ^2J(^{13}C, ^{31}P) = 6.5 Hz, OCH), 24.2 [d, ^3J(^{13}C–O–C–^{31}P) = 3 Hz, CCH_3], 24.1 [d, ^3J(^{13}C–O–C–^{31}P) = 3 Hz, CCH_3]. **^{31}P{^{1}H} NMR** (162 MHz, CD_2Cl_2): δ 16.3 (s). **Elemental analysis** calcd. for $C_{17}H_{31}Br_4NO_6P_2Sn_2$ (786.84 g/mol: C 21.17, H 3.24, N 1.45%, found: C, 21.4, H 3.3, N 1.4%.

$$[\mathbf{2}\text{-}\{\mathbf{P(O)(O}i\mathbf{Pr})_2\}\text{-}\mathbf{6}\text{-}\{\mathbf{P(O)Ph(O}i\mathbf{Pr})_2\}\mathbf{C_5H_3NSnCl}]\mathbf{SnCl_3} \quad (3)$$

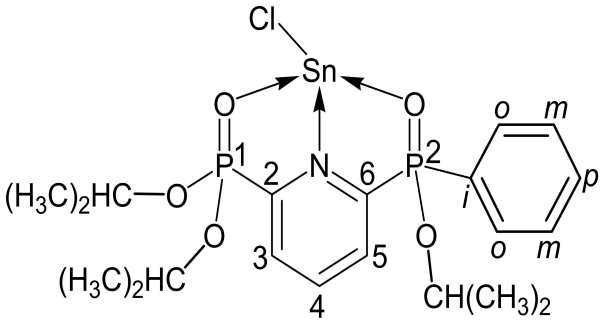

Numbering scheme for compound 3. The $SnCl_3^-$ is omitted.

Isolated as a colourless crystals of m.p. 114 °C; **^{1}H NMR** (400.25 MHz, CD_2Cl_2): δ 8.60 (m, 1H, H4), 8.27 (dd, 2H, H3/5), 8.15 (dd, 2H, H_o), 7.74 (m, 1H, H_p), 7.64 (m, 2H, H_m), 4.91 − 5.07 (complex pattern, 3H, OC*H*), 1.52 [d, 3H, ^3J(^{1}H–C–C–^{1}H) = 6 Hz, CH_3], 1.50 [d, 3H, ^3J-(^{1}H–C–C–^{1}H) = 6 Hz, CH_3], 1.46 (d, 3H, ^3J(^{1}H–C–C–^{1}H) = 6 Hz, CH_3), 1.37 [d, 3H, ^3J(^{1}H–C–C–^{1}H) = 6 Hz, CH_3], 1.33 (d, 3H, ^3J(^{1}H–C–C–^{1}H) = 6 Hz, CH_3), 1.27 (d, 3H, ^3J(^{1}H–C–C–^{1}H) = 6 Hz, CH_3); **^{13}C{^{1}H} NMR** (100.64 MHz, CD_2Cl_2): δ 150.1 [dd, ^1J(^{13}C-^{31}P) = 147 Hz, ^3J(^{13}C–^{31}P) = 18 Hz, C6], 148.3 [dd, ^1J(^{13}C-^{31}P) = 216 Hz, ^3J(^{13}C–^{31}P) = 15 Hz, C2], 142.9 (dd, ^3J(^{13}C–C–C–31P) = 9 Hz, C4,), 135.3 (d, ^4J(^{13}C–^{31}P) = 3 Hz, C_p), 133.5 [dd, ^2J(^{13}C–C–^{31}P) = 21 Hz, ^4J(^{13}C-^{31}P) = 3 Hz, C3 or C5], 133.1 (d, ^2J(^{13}C–C–^{31}P) = 12 Hz, C_o), 132.6 [dd, ^2J(^{13}C–C-^{31}P) = 19 Hz, ^4J(^{13}C-^{31}P) = 2 Hz, C3 or C5), 129.9 (d, ^3J(^{13}C-^{31}P) = 15 Hz, C_m), 125.2 [d, ^1J(^{13}C-^{31}P) = 152 Hz, C_i], 77.3 (m, OCH), 24.6 [d, ^3J(^{13}C–C–O–^{31}P) = 3 Hz, 1 C, OCHCH_3], 23.85-24.20 (superimposed resonances for five OCHCH_3 carbon atoms); **^{31}P{^{1}H} NMR** (162.0 MHz, CD_2Cl_2): δ 36.7 [s, ^1J(^{31}P-^{13}C) = 146 Hz, P2], 15.8 [s, ^1J(^{31}P–^{13}C) = 216 Hz, P1]; **^{31}P{^{1}H} NMR** (162.0 MHz, CD_2Cl_2, T = 193 K): δ 37.4 [s, P2], 36.7 [s, P2], 17.0 [s, ^1J(^{31}P–^{13}C) = 211 Hz, P1]; **^{119}Sn{^{1}H} NMR** (149.25 MHz, CD_2Cl_2, T = 193 K): δ = −89 (s, *Sn*Cl_3^-), −673 (s, *Sn*Cl^+), −680 (s, *Sn*Cl^+); **IR spectroscopy**: $\tilde{\nu}_{(P=O)=}$1157, 1174 cm^{-1}; **Elemental analysis** calcd. for $C_{20}H_{30}Cl_4NO_5P_2Sn_2$ (786.84 g/mol): C 29.82, H 3.75, N 1.74%, found: C 29.9, H 3.7, N, 1.6%.

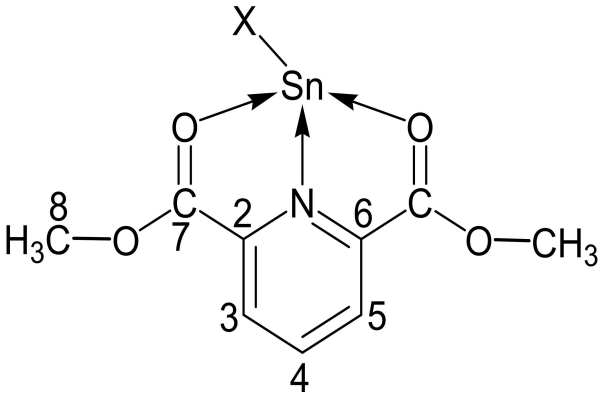

Numbering scheme for compounds 4 (X=Cl) and 5 (X=Br). The $SnX3^-$ is omitted.

$$[\mathbf{2,6}\text{-}\{\mathbf{C(O)(OMe)_2}\}\mathbf{C_5H_3NSnCl}]\mathbf{SnCl_3} \quad (4)$$

Isolated from its solution in acetonitrile as yellow crystals of m.p. 113 °C. **^{1}H NMR** (400.25 MHz, CD_2Cl_2): δ = 8.31 (d, ^3J (^{1}H–C–C–^{1}H) = 7.6 Hz 2H, H3,5), 8.08 (t, ^3J (^{1}H–C–C–^{1}H) = 7.5 Hz, 1H, H4), 4.02 (s, 6H, CH_3); **^{13}C{^{1}H} NMR** (100.64 MHz, CD_2Cl_2): δ = 165.9 (C7), 148.2 (C2), 139.5 (C4), 128.8 (C3,5), 53.8 (C8); **^{119}Sn{^{1}H} NMR** (149.25 MHz, CD_2Cl_2 T = 298 K): no signal observed; **IR spectroscopy**: $\tilde{\nu}_{C=O}$

$=1681$, 1667 cm^{-1}; **Elemental analysis** calcd. for **4**·CH3CN, $C_{11}H_{12}Cl_4N_2O_4Sn_2$ (615.46 g/mol): C 21.47, H 1.97, N 4.55 %, found: C 21.6, H 2.0, N 4.6 %.

[2,6-{C(O)OMe}C_5H_3NSnBr]$SnBr_3$ (5)

Isolated from its solution in acetonitrile as yellow crystals of m.p. 94 °C. **^{1}H NMR** (400.25 MHz, CD_3CN): $\delta = 8.61–8.67$ (complex pattern, 3H, H3,5 + H4), 4.26 (s, 6H, OCH_3); **^{13}C{^{1}H} NMR** (100.64 MHz, CD_3CN): $\delta = 167.0$ (C7), 147.5 (C2), 140.0 (C4), 129.1 (C3,5), 54.6 (C8); **^{119}Sn {^{1}H} NMR** (149.25 MHz, CD_2Cl_2, T = 298 K): no resonances were observed; **IR spectroscopy**: $\tilde{\nu}_{C=O} = 1664$ (s), 1679 (s); **Elemental analysis** calcd. for $C_9H_9Br_4NO_4Sn_2 \cdot CH_3CN$ (791.56 g/mol): C 16.66, H 1.52, N 3.53 %, found: C 16.3, H 1.4, N 3.5 %.

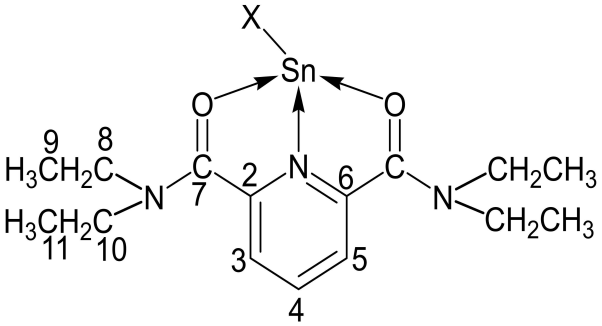

Numbering scheme for compounds 6 (X=Cl) and 7 (X=Br). The SnX_3^- is omitted.

[2,6-{C(O)(NEt)$_2$}C_5H_3NSnCl]$SnCl_3$ (6)

Isolated as colourless crystals. No melting point was determined. **^{1}H NMR** (600.29 MHz, CD_3CN): $\delta = 8.56$ (t, ^3J (^{1}H–C–C–^{1}H) = 8 Hz, 1H, H4), 8.28 (d, ^3J (^{1}H–C–C–^{1}H) = 8 Hz, 2H, H3), 3.81 (q, ^3J (^{1}H–C–C–^{1}H) = 7 Hz, 4H, NCH_2), 3.72 (q, ^3J (^{1}H–C–C–^{1}H) = 7 Hz, 4H, NCH_2), 1.49 (t, ^3J (^{1}H–C–C–^{1}H) = 7 Hz, 6H, CH_3), 1.33 (t, ^3J (^{1}H–C–C–^{1}H) = 7 Hz, 6H, CH_3); **^{13}C{^{1}H} NMR** (150.94 MHz, CD_3CN, 298 K): $\delta = 167.8$ (C7), 146.8 (C2, C6), 144.4 (C4), 129.7 (C3, C5), 46.4 (C8), 44.8 (C10), 13.9 (C9), 12.3 (C11); **^{119}Sn{^{1}H} NMR** (149.25 MHz, CD_2Cl_2, T = 298 K): $\delta = -35$ ($\nu_{1/2}$ ~6000 Hz) and −523 ($\nu_{1/2}$ ~7000 Hz).

Elemental analysis calcd. for $C_{15}H_{23}Cl_4N_3O_2Sn_2$ (656.6 g/mol): C 27.44, H 3.53, N 6.40 %, found: C 27.1, H 3.7, N 6.6 %.

[2,6-{C(O)(NEt)$_2$}C_5H_3NSnBr]$SnBr_3$ (7)

Isolated as a yellow solid of m.p. 136 °C. No elemental analysis was performed. The crystal actually measured by X-ray diffraction analysis proved to be complex **7**.

Synthesis of 2-[P(O)(OiPr)$_2$-6-{P(O)(OiPr)OSnCl}]$C_5H_3N \cdot SnCl_2$) (8)

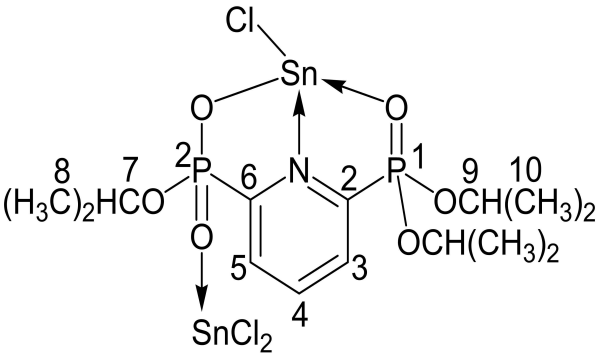

Numbering scheme for compound 8

A toluene solution of **1** (0.80 g, 1 mmol) was heated for 16 h at 80 °C. The reaction mixture was filtered and the volatiles were removed under reduced pressure to obtain a colourless solid. The latter was recrystallized a small amount of single crystals suitable for X-ray diffraction measurements. **^{1}H NMR** (400.25 MHz, C_6D_6): $\delta =$ 8.03 (m, 1H, H4), 7.30 (m, 1H, H3/5), 7.13 (m, 1H, H3/5), 4.92 (m, 3H, OC*H*), 1.14 (d, 12H, ^3J(^{1}H–C–C–^{1}H) = 6 Hz, CH_3), 0.94 (d, 6H, ^3J(^{1}H–C–C–^{1}H) = 6 Hz, CH_3); **^{13}C{^{1}H} NMR** (100.64 MHz, C_6D_6): $\delta =$ 153.4 [dd, ^1J(^{13}C-^{31}P) = 200 Hz, ^3J(^{13}C–N-C-^{31}P) = 16 Hz, C2], 146.6 [dd, ^1J(^{13}C-^{31}P) = 209, ^3J(^{13}C–N–C-^{31}P) = 16 Hz, C6], 140.0 [t, ^3J-(^{13}C–C–C–^{31}P) = 9 Hz, C4],, 133.0 [dd, ^2J(^{13}C–C-^{31}P) = 19 Hz, ^4J(^{13}C–C-C–C-^{31}P) = 3 Hz, C3], 130.5 [dd, ^2J(^{13}C–C-^{31}P) = 19 Hz, ^4J-(^{13}C–C–C–C–^{31}P) = 3 Hz, C5], 75.4 [d, ^2J(^{13}C–O–^{31}P) = 5 Hz, C9], 73.2 (d, ^2J(^{13}C–O-^{31}P) = 6 Hz, C7), 23.9 (d, ^3J(^{13}C–O–C–^{31}P) = 3 Hz, CH_3), 23.6 (d, ^3J(^{13}C–O–C–C–^{31}P) = 6 Hz, CH_3); **^{31}P{^{1}H} NMR** (162.02 MHz) C_6D_6, T = 298 K): $\delta = 18.3$ [^1J(^{31}P-^{13}C) = 211 Hz, P1], 13.4 [^1J(^{31}P-^{13}C) = 201 Hz, P2], Toluene-d_8,T = 193 K: $\delta = 17.8$ [J(^{31}P–O–$^{117/119}$Sn) = 53 Hz, P1], 12.2 [J(^{31}P–O-$^{117/119}$Sn) = 89 Hz, P2] ; **^{119}Sn{^{1}H} NMR** (149.25 MHz, C_6D_6, T = 298 K): $\delta = -587$ and −208, Toluene-d_8, T = 193 K: and δ −639 ($\nu_{1/2}$ ~500 Hz) and −267 ($\nu_{1/2}$ ~600 Hz); No elemental analysis was performed.

Synthesis of [2-{P(O)(OiPr)Ph}-6-{P(OSnCl$_2$)(OiPr)OSnCl}]C_5H_3N (9)

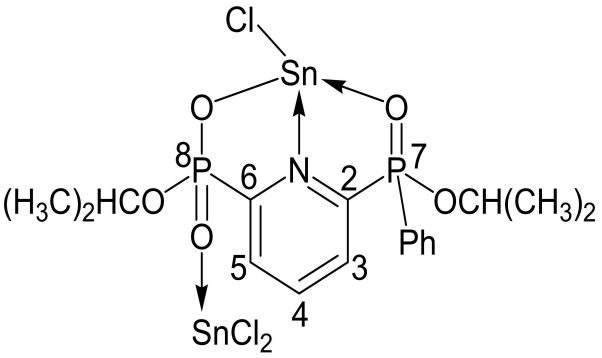

Numbering scheme for compound 9

A toluene solution of **3** (0.64 g, 0.8 mmol) was heated for 16 h at 80 °C. The reaction mixture was filtered and the volatiles were removed under reduced pressure to obtain a solid material. By recrystallization from toluene a few colourless crystals of **9** suitable for X-ray diffraction analysis were obtained. There was not enough material to perform elemental analysis and to record NMR spectra. The crystal actually measured proved to be compound **9**.

Synthesis of $[\{2\text{-}C(O)OMe\text{-}6\text{-}C(O)OSnCl\}C_5H_3N]$ (10)

$[C_5H_3N\text{-}2,6\text{-}\{C(O)O\}_2Sn(OSMe_2)_2]$ (11)

and

$[C_5H_3N\text{-}2,6\text{-}\{C(O)O\}_2Sn(OSMe_2)]$ (12)

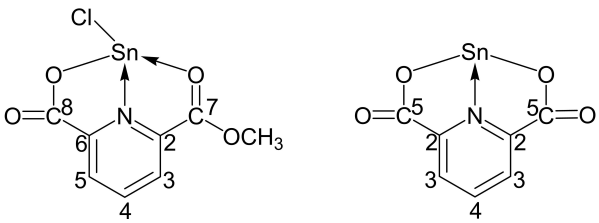

Numbering schemes for compounds 10 (left) and 11/12 (right, without coordinated DMSO)

Compound **4** (1.94 g, 3.16 mmol) was suspended in toluene (20 mL) and heated for 16 h at reflux. In course of this time the suspended material changed its colour from yellow to white. After cooling the reaction mixture to room temperature, it was filtered giving 1.65 g dry residue. The residue was suspended in 20 mL acetonitrile (ACN) and heated to reflux for 15 min followed by filtration. The filtrate was stored in the freezer (T = −19 °C) giving 131 mg (yield 12%) of compound **10** (m.p. 222–225 °C) as crystalline material.

^{1}H NMR (400.25 MHz, CD_3CN, 298 K): δ = 8.47-8.57 (complex pattern, 3H, H3, H4, H5), 4.16 (s, 3H, OCH_3). **^{119}Sn{^{1}H} NMR** (149.25 MHz, CD_3CN): no resonance was observed. **IR spectroscopy**: $\tilde{\nu}_{C=O=}$1589, 1660, 1718 cm^{-1}. **ESI-MS** (70 eV, positive mode): m/z (%) 335.9073 [$C_8H_7ClNO_4Sn^+$] (calcd 335.9075); **Elemental analysis**: calcd. for $C_8H_6ClNO_4Sn$ (334.30 g/mol): C 28.74, H 1.81, N 4.19, found: C 28.0, H 1.8, N 4.4%.

Part of the solid residue was dissolved in DMSO/THF and the solution was stored in the fridge (T = 4 °C). After 10 days, crystals of **11** (100 mg, triclinic modification) had been formed.

The second part of the solid residue was dissolved in DMSO only. After one day at room temperature, crystals of the orthorhombic modification of **11** (300 mg) had been formed. The total yield of **11** is 29%. Both modifications do not melt until 340 °C.

^{1}H NMR (400.25 MHz, DMSO, C_6D_6, 298 K): δ = 8.16–8.27 (complex pattern, 3H, H3, H4). The signal for the SCH_3 protons is superimposed with the resonance for the DMSO protons at δ 2.32. **^{13}C{^{1}H} NMR** (100.64 MHz, DMSO/C_6D_6): δ = 166.4 (C5), 146.0 (C2), 143.9 (4), 126.1 (3). The signal for the SCH_3 carbon atoms is superimposed with the resonance for the DMSO carbon atoms at δ 40.8. **^{119}Sn{^{1}H} NMR** (149.25 MHz, DMSO/C_6D_6): no resonance was observed. **IR spectroscopy**: $\tilde{\nu}_{C=O}$ = 1659, 1636, 1592 cm^{-1}.

Elemental analysis: calcd. for $C_{11}H_{15}NO_6S_2Sn$ (440.08 g/mol): C 30.02, H 3.44, N 3.18 found: C 30.0, H 3.5, N 3.2%.

In a second experiment, some crystals of the mono-DMSO-coordinated $[C_5H_3N\text{-}2,6\text{-}\{C(O)O\}_2Sn(OSMe_2)]$ (**12**) were obtained from DMSO/THF (1:1 mixture) as greenish crystals of m.p > 340 °C.

IR spectroscopy: $\tilde{\nu}_{C=O}$ = 1666, 1609 cm^{-1}.

Elemental analysis: calcd. For $C_9H_9NO_5SSn$ (361.95 g/mol): C 29.87, H 2.51, N 3.87 found: C 29.3, H 2.7, N 3.7%.

$[2,6\text{-}\{P(O)(OiPr)_2\}C_5H_3NSnCl]SnCl_3 \cdot W(CO)_4$ (13)

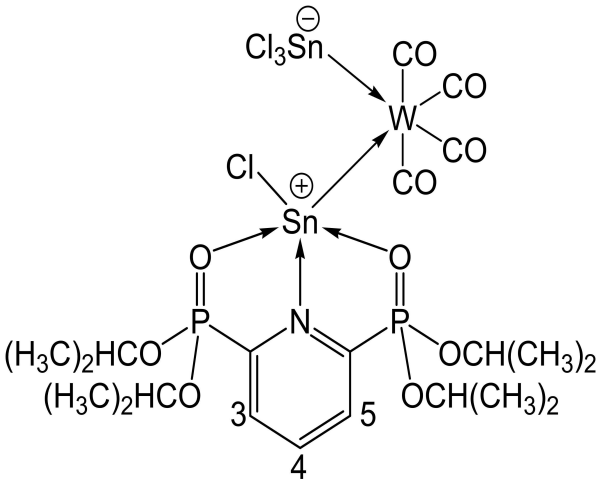

Numbering scheme for compound 13

To a solution of tungsten pentacarbonyl-THF complex in THF, generated from $W(CO)_6$ (1.00 g, 2.84 mmol) by irradiation with UV-light, was added compound **1** (2.23 g, 2.84 mmol). The reaction mixture was stirred for 18 h. A ^{31}P{^{1}H} NMR spectrum of the reaction mixture showed a signal at δ 13.4 ppm. The yellow solution was evaporated in vacuo to dryness and the residual $W(CO)_6$ was sublimated in vacuo. The residue was dissolved in THF and after storage of this solution for one month a few colourless single crystals of **13** suitable for X-ray diffraction analysis had been formed. No melting point was determined and no elemental analysis was performed.

^{1}H NMR (400.25 MHz, CD_2Cl_2): δ = 8.25 (complex pattern, 1H, H4), 8.13 (complex pattern, 2H, H3,5), 4.87 (m, 4H, OCH), 1.28 (d, ^3J (^{1}H–C–C–^{1}H) = 6.1 Hz, 12H, CCH_3), 1.13 (d, ^3J (^{1}H–C–C–^{1}H) = 6.2 Hz, 12H, CCH_3). **^{31}P{^{1}H} NMR** (162 MHz, CD_2Cl_2): δ = 13.4 (s).

Literature

Part of this work was first presented at the 18. Vortragstagung der Wöhler Vereinigung für Anorganische Chemie, 26.-28. September, 2016, Berlin, Book of Abstracts P084 (Supporting Information, Figures S82 and S83).

Acknowledgements

We thank the Regional Computing Centre of the University of Cologne (RRZK) for providing computing time on the DFG-funded High Performance Computing (HPC) system CHEOPS as well as support. A. H. thanks Prof. Dr. S. Herres-Pawlis for valuable support und fruitful discussions. T. R. gratefully acknowledges the German Academic Exchange Board (DAAD) for a scholarship. We thank Mr. Markus Hüffner for performing the elemental analyses. We cordially thank the anonymous reviewers for helpful comments. Open Access funding enabled and organized by Projekt DEAL.

Conflict of Interests

The authors declare no conflict of interest.

Data Availability Statement

The data that support the findings of this study are available in the supplementary material of this article.

Keywords: Tin cation · X-ray diffraction · tungsten tetracarbonyl complex · DFT calculations · ester cleavage

[1] a) M. Asay, C. Jones, M. Driess, *Chem. Rev.* **2011**, *111*, 354–396; b) K. Izod, *Coord. Chem. Rev.* **2012**, *256*, 2972–2993; c) S. K. Mandal, H. W. Roesky, *Chem. Commun.* **2010**, *46*, 6016–6041; d) Y. Mizuhata, T. Sasamori, N. Tokitoh, *Chem. Rev.* **2009**, *109*, 3479–3511; e) P. P. Power, *Chem. Rev.* **1999**, *99*, 3463–3504; f) N. Tokitoh, R. Okazaki, *Coord. Chem. Rev.* **2000**, *210*, 251–277; g) T. A. Engesser, M. R. Lichtenthaler, M. Schleep, I. Krossing *Chem. Soc. Rev.* **2016**, *45*, 789–899.

[2] a) A. Schäfer, W. Saak, D. Haase, T. Müller, *Chem. Eur. J.* **2009**, *15*, 3945–3950; b) P. P. Gaspar In *Organosilicon Chemistry VI*; N. Auner, J. Weis, Eds.; Wiley-VCH: Weinheim, Germany, 2005; Vol. 2, p 10–25.

[3] a) F. X. Kohl, P. Jutzi, *Chem. Ber.* **1981**, *114*, 488–494; b) P. Jutzi, F. Kohl, C. Krüger, G. Wolmershäuser, P. Hofmann, P. Stauffert, *Angew. Chem.* **1982**, *94*, 66–67; c) F. Kohl, E. Schlüter, P. Jutzi, C. Krüger, G. Wolmershäuser, P. Hofmann, P. Stauffert, *Chem. Ber.* **1984**, *117*, 1178–1193; d) P. Jutzi, B. Hampel, *Organometallics* **1986**, *5*, 730–734; e) P. Jutzi, *Adv. Organomet. Chem.* **1986**, *26*, 217–295; f) P. Jutzi, A. Mix, B. Rummel, W. W. Schoeller, B. Neumann, H.-G. Stammler, *Science* **2004**, *305*, 849–851.

[4] P. A. Rupar, R. Bandyopdhayay, B. F. T. Cooper, M. R. Stinchcombe, P. J. Ragogna, C. L. B. Macdonald, K. M. Baines, *Angew. Chem. Int. Ed.* **2009**, *48*, 5155–5158.

[5] I. Objartel, H. Ott, D. Stalke, *Z. Anorg. Allg. Chem.* **2008**, *634*, 2373–2379.

[6] a) A. P. Singh, H. W. Roesky, E. Carl, D. Stalke, J.-P. Demers, A. Lange, *J. Am. Chem. Soc.* **2012**, *134*, 4998–5003; b) M. Bouška, L. Dostál, M. Lutter, B. Glowacki, Z. Růžičková, D. Beck, R. Jambor, K. Jurkschat, *Inorg. Chem.* **2015**, *54*, 6792–6800; c) J. Flock, B. Steller, P. Unger, B. Gerke, R. Pöttgen, R. C. Fischer, *Z. Naturforsch.* **2017**, *72*, 883–894.

[7] a) M. Bouška, L. Dostál, A. Růžička, R. Jambor, *Organometallics* **2013**, *32*, 1995–1999; b) M. Novák, J. Turek, Y. Milasheuskaya, Z. Růžičková, Š. Podzimek, R. Jambor *Dalton Trans.* **2021**, *50*, 16039–16052; c) R. K. Raut, P. Sahoo, D. Chimnapure, M. Majumdar, *Dalton Trans.* **2019**, *48*, 10953–10961.

[8] C. Gurnani, A. L. Hector, E. Jager, W. Levason, D. Pugh, G. Reid, *Dalton Trans.* **2013**, *42*, 8364–8374.

[9] a) M. Gawron, C. Dietz, M. Lutter, A. Duthie, V. Jouikov, K. Jurkschat, *Chem. Eur. J.* **2015**, *21*, 16609–16622; b) T. J. Hadlington, A. Kostenko, M. Driess, *Chem. Eur. J.* **2021**, *27*, 2476–2482; c) R. Baierl, A. Kostenko, F. Hanusch, S. Inoue, *Dalton Trans.* **2021**, *50*, 14842–14848;d) F. S. Tschernuth, F. Hanusch, T. Szilvási, S. Inoue, *Organometallics* **2020**, *39*, 4265–4272; e) A. Hinz, *Chem. Eur. J.* **2019**, *25*, 3267–3271; f) H. V. R. Dias, W. Jin, *J. Am. Chem. Soc.* **1996**, *118*, 9123–9126; g) M. J. Taylor, A. J. Saunders, M. P. Coles, J. R. Fulton, *Organometallics* **2011**, *30*, 1334–1339; h) P. A. Gray, K. D. Krause, N. Burford, B. O. Patrick, *Dalton Trans.* **2017**, *46*, 8363–8366; i) S. Khan, G. Gopakumar, W. Thiel, M. Alcarazo, *Angew. Chem. Int. Ed.* **2013**, *52*, 5644–5647; j) J. Li, Ch. Schenk, F. Winter, H. Scherer, N. Trapp, A. Higelin, S. Keller, R. Pöttgen, I. Krossing, C. Jones, *Angew. Chem.* **2012**, *124*, 9695–9699; *Angew. Chem. Int. Ed.* **2012**, *51*, 9557–9561; k) Ch. L. B. Macdonald, R. Bandyopadhyay, B. F. T. Cooper, W. W. Friedl, A. J. Rossini, R. W. Schurko, S. H. Eichhorn, R. H. Herber, *J. Am. Chem. Soc.* **2012**, *134*, 4332–4345; l) J. C. Avery, M. A. Hanson, R. H. Herber, K. J. Bladek, P. A. Rupar, I. Nowik, Y. Huang, K. M. Baines, *Inorg. Chem.* **2012**, *51*, 7306–7316; m) S. Nasemann, R. Franz, D. Kargin, C. Bruhn, Z. Kelemen, T. Gutmann, R. Pietschnig, *Chem. Asian J.* **2024**, *19*, e202300950.

[10] a) T. Zöller, L. Iovkova-Berends, T. Berends, C. Dietz, G. Bradtmöller, K. Jurkschat, *Inorg. Chem.* **2011**, *50*, 8645–8653; b) M. Wagner, T. Zöller, W. Hiller, M. H. Prosenc, K. Jurkschat, *Chem. Commun.* **2013**, *49*, 8925–8927; c) M. Wagner, T. Zöller, W. Hiller, M. H. Prosenc, K. Jurkschat, *Chem. Eur. J.* **2013**, *19*, 9463–9467; d) M. Wagner, C. Dietz, M. Bouška, L. Dostál, Z. Padělková, R. Jambor, K. Jurkschat, *Organometallics* **2013**, *32*, 4973–4984; e) S. Krabbe, M. Wagner, C. Löw, C. Dietz, M. Schürmann, A. Hoffmann, S. Herres-Pawlis, M. Lutter, K. Jurkschat, *Organometallics* **2014**, *33*, 4433–4441; f) B. Nayyar, H. Alnasr, W. Hiller, K. Jurkschat, *Angew. Chem. Int. Ed.* **2018**, *57*, 5544–5547.

[11] a) R. Sevcik, M. Necas, J. Novosad, *Polyhedron* **2003**, *22*, 1585–1593; b) E. A. Konopkina, P. I. Matveev, P.-W. Huang, A. A. Kirsanova, M. G. Chernysheva, T. B. Sumyanova, K. S. Domnikov, W.-Q. Shi, S. N. Kalmykov, V. G. Petrov, N. E. Borisova, *Dalton Trans.* **2022**, *51*, 11180–11192; c) M. Novák, J. Turek, Y. Milasheuskaya, M. Syková, Libor Dostál, J. Stalmans, Z. Růžičková, K. Jurkschat, R. Jambor, *Dalton Trans.* **2023**, *52*, 2749–2761; d) S. Stigler, S. Fujimori, A. Kostenko, S. Inoue, *Chem. Sci.* DOI: 10.1039/d3sc06452b; e) Y. Belabassi, S. Alzghari, J.-L. Montchamp, *J. Organomet. Chem.* **2008**, *693*, 3171–3178.

[12] a) A. Bondi, *J. Phys. Chem.* **1964**, *68*, 441–451; b) M. Mantina, A. C. Chamberlin, R. Valero, C. J. Cramer, D. G. Truhlar, *J. Phys. Chem. A* **2009**, *113*, 5806–5812; c) P. Pyykkö, M. Atsumi, *Chem. Eur. J.* **2009**, *15*, 186–197; d) G. R. Desiraju, P. S. Ho, L. Kloo, A. C. Legon, R. Marquardt, P. Metrangolo, P. Politzer, G. Resnati, K. Rissanen, *Pure Appl. Chem.* **2013**, *85*, 1711–1713; e) G. Cavallo, P. Metrangolo, R. Milani, T. Pilati, A. Priimagi, G. Resnati, G. Terraneo, *Chem. Rev.* **2016**, *116*, 2478–2601; f) F. Otte, J. Kleinheider, B. Grabe, W. Hiller, F. Busse, R. Wang, N. M. Kreienborg, C. Merten, U. Englert, C. Strohmann, *ACS Omega* **2023**, *8*, 21531–21539.

[13] F. Richter, M. Dargatz, H. Hartung, D. Schollmeyer, H. Weichmann, *J. Organomet. Chem.* **1996**, *514*, 233–241.

[14] a) M. Henn, V. Deáky, S. Krabbe, M. Schürmann, M. H. Prosenc, S. Herres-Pawlis, B. Mahieu, K. Jurkschat, *Z. Anorg. Allg. Chem.* **2011**, *637*, 211–223; b) I. Barbul, R. A. Varga, C. Silvestru, *Acta Crystallogr.* **2011**, *E67*, m486; c) M. Gielen, E. Joosen, T. Mancilla, K. Jurkschat, R. Willem, C. Roobol, J. Bernheim, G. Atassi, F. Huber, E. Hoffman, H. Preut, B. Mahieu, *Main Group Met. Chem.* **1987**, *10*, 147–167; d) F. Huber, H. Preut, E. Hoffmann, *Acta Crystallogr.* **1989**, *C45*, 51–54; e) A. Szorcsik, L. Nagy, J. Sletten, G. Szalontai, E. Kamu, T. Fiore, L. Pellerito, E. Kalman, *J. Organomet. Chem.* **2004**, *689* 1145–1154; f) S. W. Ng, *Acta Crystallogr.* **2011**, *E67*, m277; g) T. Diop, A. Ndioléne, M. B. Diop, M. S. Boye, A. van der Lee, F. Dumitru, C. A. K. Diop, M. Sidibé, *Z. Naturforsch.* **2021**, *76(2)b*, 127–132; h) A. C. Doriguetto, J. Ellena, *Spectrochim. Acta Part A* **2005**, *61*; i) C. Ma, J. Li, R. Zhang, D. Wang, *Inorg. Chim. Acta* **2005**, *358*, 4575–4580.

[15] T. Berends, L. Iovkova, G. Bradtmöller, I. Oppel, M. Schürmann, K. Jurkschat, *Z. Anorg. Allg. Chem.* **2009**, *635*, 369–374.

[16] a) E. D. Glendening, C. R. Landis, F. Weinhold, *J. Comput. Chem.* **2013**, *34*, 1429–1437; b) F. Weinhold, C. Landis, Valency, Bonding -A Natural Bond Orbital Donor-Acceptor Perspective, Cambridge University Press, New York, **2005**; c) E. D. Glendening, J. K. Badenhoop, A. E. Reed, J. E. Carpenter, J. A. Bohmann, C. M. Morales, C. R. Landis, F. Weinhold, *NBO 6.0*, Theoretical Chemistry Institute, University of Wisconsin: Madison, **2013**, available at: www. chem.wisc.edu/nbo6, accessed Feb. 1, 2013.

[17] a) K. Kitaura, K. Morokuma, *Int. J. Quantum Chem.* **1976**, *10*, 325–340; b) T. Ziegler, A. Rauk, *Theor. Chim. Acta* **1977**, *46*, 1–10.

[18] a) M. Tao, J. P. Perdew, V. N. Staroverov, G. E. Scuseria, *Phys. Rev. Lett.* **2003**, *91*, 146401; b) V. N. Staroverov, G. E. Scuseria, J. Tao, J. P. Perdew, *J. Chem. Phys.* **2003**, *119*, 12129 and Erratum **2004**, *121*, 11507(E).

[19] a) F. Weigend, R. Ahlrichs, *Phys. Chem. Chem. Phys.* **2005**, *7*, 3297–305; b) A. Schäfer, C. Huber, R. Ahlrichs, *J. Chem. Phys.* **1994**, *100*, 5829–5835; c) K. Eichkorn, F. Weigend, O. Treutler, R. Ahlrichs, *Theor. Chem. Acc.* **1997**, *97*, 119–124; d) F. Weigend, M. Häser, H. Patzelt, R. Ahlrichs, *Chem. Phys. Lett.* **1998**, *294*, 143–152; e) F. Weigend, F. Furche, R. Ahlrichs, *J. Chem. Phys.* **2003**, *119*, 12753–12762.

[20] ECP for Sn: a) B. Metz, H. Stoll, M. Dolg, *J. Chem. Phys.* **2000**, *113*, 2563–2569 and ECP for W:; b) D. Andrae, U. Haeussermann, M. Dolg, H. Stoll, H. Preuss, *Theor. Chim. Acta* **1990**, *77*, 123–141.

[21] a) S. Grimme, S. Ehrlich, L. Goerigk, *J. Comput. Chem.* **2011**, *32*, 1456–1465; b) L. Goerigk, S. Grimme, *Phys. Chem. Chem. Phys.* **2011**, *13*, 6670–6688; c) For TPSSh, the values of the original paper have been substituted by the corrected values kindly provided by S. Grimme as private communication and published in; d) A. Hoffmann, R. Grunzke, S. Herres-Pawlis, *J. Comput. Chem.* **2014**, *35*, 1943–1950.

[22] a) T. Zöller, C. Dietz, F. Winter, R. Pöttgen, S. I. Gorelsky, A. Hoffmann, S. Herres-Pawlis, K. Jurkschat, *Chem. Eur. J.* **2018**, *24*, 5551–5561; b) F. Richter, J. Weikard, K. Jurkschat, B. Glowacki, H. Alnasr, A. Platzek, WO 2019('011957A1: **2019**.

[23] W. L. F. Armarego, C. L. L. Chai, *Purification of laboratory chemicals* Elsevier/Butterworth-Heinemann, Amsterdam, Boston, **2009**.
[24] J. Zhou, B. Li, Z.-C. Qian, B.-F. Shi, *Adv. Synth. Catal.* **2014**, *356*, 1038–1046.
[25] G. R. Fulmer, A. J. M. Miller, N. H. Sherden, H. E. Gottlieb, A. Nudelman, B. M. Stoltz, J. E. Bercaw, K. I. Goldberg, *Organometallics* **2010**, *29*, 2176–2179.
[26] G. M. Sheldrick, *Acta Crystallogr.* **1990**, *A46*, 467.
[27] G. M. Sheldrick, *SHELXL2018, Acta Cryst.* **2015**, *C71*, 3–8.
[28] *International Tables for X-Ray Crystallography*, Dortrecht, Kluwer Academic Publishers.
[29] Gaussian 16, Revision C.01, M. J. Frisch, G. W. Trucks, H. B. Schlegel, G. E. Scuseria, M. A. Robb, J. R. Cheeseman, G. Scalmani, V. Barone, G. A. Petersson, H. Nakatsuji, X. Li, M. Caricato, A. V. Marenich, J. Bloino, B. G. Janesko, R. Gomperts, B. Mennucci, H. P. Hratchian, J. V. Ortiz, A. F. Izmaylov, J. L. Sonnenberg, D. Williams-Young, F. Ding, F. Lipparini, F. Egidi, J. Goings, B. Peng, A. Petrone, T. Henderson, D. Ranasinghe, V. G. Zakrzewski, J. Gao, N. Rega, G. Zheng, W. Liang, M. Hada, M. Ehara, K. Toyota, R. Fukuda, J. Hasegawa, M. Ishida, T. Nakajima, Y. Honda, O. Kitao, H. Nakai, T. Vreven, K. Throssell, J. A. Montgomery, Jr., J. E. Peralta, F. Ogliaro, M. J. Bearpark, J. J. Heyd, E. N. Brothers, K. N. Kudin, V. N. Staroverov, T. A. Keith, R. Kobayashi, J. Normand, K. Raghavachari, A. P. Rendell, J. C. Burant, S. S. Iyengar, J. Tomasi, M. Cossi, J. M. Millam, M. Klene, C. Adamo, R. Cammi, J. W. Ochterski, R. L. Martin, K. Morokuma, O. Farkas, J. B. Foresman, D. J. Fox, Gaussian, Inc., Wallingford CT, **2019**.
[30] a) S. I. Gorelsky, AOMix: Program for Molecular Orbital Analysis, version 6.87, University of Ottawa, 2014, http://www.sg-chem.net/;b) S. I. Gorelsky, A. B. P. Lever, *J. Organomet. Chem.* **2001**, *635*, 187–196.

Manuscript received: February 12, 2024
Accepted manuscript online: June 4, 2024
Version of record online: July 26, 2024